Optimization of process conditions for maximum metal recovery from spent zinc-manganese Batteries: Illustration of Statistical based Automated Neural Network approach

[1] C. Ruhatiya, [2]Su Shaosen, [3]Chin-Tsan Wang, A.K Jishnu[4], [5,6*]Yogesh Bhalerao

[1]School of Engineering Sciences, Mahindra École Centrale, Hyderabad, Telangana 500043, India
[2]Intelligent Manufacturing Key Laboratory of Ministry of Education, Shantou University, Shantou, China
[3]Department of Mechanical and Electro-Mechanical Engineering, National I Lan University, ILan, Taiwan
[4]School of Mechanical Sciences, Indian Institute of Technology, Bhubaneswar, India
[5]Department of Mechanical Engineering, MIT Academy of Engineering (MAE), Pune MH 412105, India
[6]Engineering Faculty of Science, University of East Anglia, Norwich Research Park, Norwich NR47TJ

Abstract

Recovery of the vital metals from spent batteries using bioleaching is one of the commonly used method for recycling of spent batteries. In this study, a Statistical based Automated Neural Network approach is proposed for determination of optimum input parameters values in bioleaching of zinc-manganese batteries. Experiments are performed to measure the recovery of zinc and manganese based on the input parameters such as energy substrates concentration, pH control of bioleaching media, incubating temperature and pulp density. It was found that the proposed model based metal extraction models precisely estimated the yields of zinc and manganese with higher values of coefficient of determination of 0.94. Based on global sensitivity analysis, it was found that for the extraction of zinc, the most contributing parameters are pulp density and pH while for extraction of Mn the most contributing parameters are pulp density and incubating temperature. The optimum parameter values for maximum recovery of zinc and maximum recovery of manganese are determined using optimization method of simulated annealing. The optimum parameter values obtained for maximum recovery of Zn metal are as substrates concentration 32 g/L, pH 1.9-2.0, incubating temperature 30 ℃, pulp density 10% and substrates concentration 32 g/L, pH 2.0, incubating temperature 35 ℃, pulp density 8% for maximum recovery of Mn.

Keywords: Recycling; bioleaching process; Optimization; metals recovery; Statistical based Automated Neural Network;

Novel optimization method for recycling batteries

Email*: ybhalerao@maepune.ac.in;

1. Introduction

Electric vehicle (EV) related consumer economy is increasing tremendously worldwide. For instance, it is expected that the global battery market will cross US $100 billion mark by 2025 [1]. Further, growth in EV market is fueled by governmental measures [2]. The major producers of batteries like Lithium-ion batteries (LIBs) are centred in east Asia. As of 2015, 88% of total global LIBs cell manufacturing units and 79% of automotive LIBs manufacturing units were located in China, Japan and Korea [3]. There is a drop of 73% in price of LIBs from 2010 to 2016, these price drop is making it more consumer friendly [4]. In 2016 new Electric Vehicles (EVs) sales consumed over 20 GWh, which is one fifth of installed capacity size [4]. The primary power technology in EVs is battery packs. The Battery pack is made up of identical batteries or individual battery units connected in a pattern to give desired voltage and power density. The use of battery pack in EVs has become norm because of its compact design and it can be dismantled for recycling efficiently once it's out of use [5]. The battery pack is made up of Li-ion, Ni-Cd or Zn-Mn cells, after the battery pack is dismantled this all cells are treated individually and are grouped categorically for recycling or re-purposing [5].

There are two basic type of household batteries:- primary cells(one time use) and secondary cells(rechargeable cells). In first category, the major contributors are the zinc-carbon(Zn-C) and the alkaline -manganese batteries [6]. While in second category major contributors are Nickel-Cadmium (Ni-Cd) and Lithium-ion batteries (LIBs) [6]. This large consumption of portable batteries in last 30 years for the versatility, low cost and its requirement in electronics industry is amounting to hazardous waste [7]. Disposal of spent batteries has become an environmental issue of concern, which is needed to be improved because of the high cost of safe and environmental friendly disposal [8]. This toxic waste of spent batteries pose threat to environment. There is need of efficient and cheap recycling process for this toxic waste. The increasing concern about environmental issues in last decade has lead to the stricter regulations worldwide on hazardous residues containing heavy metal spent batteries [8]. The Ni-Cd system is considered to be one of the most hazardous in terms of disposal [9]. Nickel- metal hydride batteries (NiMH) are regarded as a suitable substitute for Ni-Cd batteries due to its environmental friendliness in many applications. However, it cannot be commercial used owing to a higher cost of manufacture compared to Ni-Cd [10]. It is reported that huge quantities of waste batteries are generated every year in China and of that great deal of waste batteries were discarded directly while great part of these spent batteries can be reused [11]. The proper disposal and extraction of the valuable metals from spent batteries is important for sustainable development [12].

The Recovery of valuable and toxic metals such as Li, Co, Zn, Ni, Cd and Mn from spent batteries is enormous area of interest for solid waste treatment [11-15]. Spent zinc-manganese batteries (ZMB) occupy the great proportion of the total spent batteries owing to its low cost and short life. Content of Zn and Mn in spent batteries is 12-28% and 26-45% respectively [16]. The physical-chemical processes such as pyrometallurgy and hydrometallurgy, which are commercially used, are already applied to remove and recover of valuable metals from spent batteries. [1,2]. But, all these physical-chemical processes are energy intensive, heavy polluting and have high security risk associated with it. Whereas, bioleaching technology comparatively has less energy consumption, and more environmental friendly [17-19]. However, it cannot be applied commercially until it is proved that using this process costs less than the application of already extensively commercial used pyro and hydrometallurgy processes. In the bioleaching process the yield of metal was strongly affected by operating environment such as energy substrates type and dose(SC), initial pH, temperature(T), and pulp density(PD) [20]. Optimization of these parameters is necessary to obtain required yield of metal from spent batteries and a proper economical setup for bioleaching which can compete with the commercial physical-chemical processes. In direct bioleaching process on spent batteries the leaching period is shortened compared to indirect process [17,19,21]. But operational pulp density was equal or less than 1% due to the toxicity of he spent batteries. When The pulp density grew from 1% to 10%, the size of leaching reactor dropped to 10%, this results in huge reduction in leaching cost [20]. In a hydrometallurgical method based on strong acid when utilized on a spent battery, the pulp density was 10% or higher [1,2,16]. Comparing to these commercial process, 10% of pulp density is required in bioleaching process on spent batteries in order to compete with physical-chemical processes. One-factor-at-a-time methodology is a basic method of the identification of the optimum settings of operating parameters [17,19,20,21]. This methodology is inefficient as it doesn't give information about interactions between parameters in process [22]. In the perspective of development of multi-variable model development, the past studies use response surface methodology (RSM) for optimizing the process conditions for extraction of metals from spent batteries[21, 23]. The assumption of model structure is the basis for the utilization of RSM in estimating the coefficients of the model. Thus, information about the process behaviour is necessary for an efficient employment of RSM. These method is very efficient if and only if the information about the system behaviour is available [23]. However, actual engineering and design problems are not that straight-forward, they are often complex and have partial information on process behaviour. For such cases RSM is not a viable tool for process modelling [24]. To address such problems a robust and efficient method is required, predictive modelling methods based on artificial intelligence are promising to address such problems with high accuracy [24-25]. Recently, some literature have reported use of evolutionary methods such as genetic algorithms (GA) for metal extraction from spent Li-ion batteries [25], these method have proved to be efficient compared to conventional modelling approach. While some literature have also reported about use of Artificial Neural Network (ANN) and Generalized Neural Network (GNN) for modelling process conditions of metal extraction from waste electronics devices[26-27]. It was reported that of all the above mentioned process GNN performed the best [27]. But, GNN is a complex network to implement, leaving it with more room for error while implementing. A more easy, generic and efficient method is needed which would give high accuracy with ease. The method implemented for modelling should not be prone to large variations in output due to small perturbations. One such method is Statistical based Automated Neural Network (SANN) [27-28]. Its ability to effectively model and improve the productivity of bioleaching process can be explored.

In the present work, a comprehensive Experimental Combined Automated Neural Network approach is proposed as shown in figure 1. Experiments are performed to measure the recovery of Zn and Mn based on the input parameters such as energy substrates concentration (SC), incubating temperature (T), pulp density (PD) and pH control of bioleaching media (pH). Statistical based Automated Neural Network (SANN) methodology is then used to optimize the bioleaching process for extraction of metals from ZMBs spent batteries by a multivariate study of parameters at higher pulp density of 8-12% to compete with already extensively used physical-chemical process. Four input parameters were evaluated to confirm their sensitivity and interactions on extraction efficiency of Zn and Mn; The resulting efficiencies are then compared with linear Analysis of Variance (ANOVA) and regression models to check the efficacy of using a SANN model. Though here ANOVA is used for the comparative analysis, but future work of authors shall be to apply sophisticated algorithms based on support vector regression, genetic programming, deep learning neural networks, probability and integrated learning [29-33].

2. Research problem statement

This section discusses the research problem on optimization of operational parameters in bioleaching process for removal of metal from spent batteries. For the competition with physical-chemical processes, the bioleaching process must be optimized in such a way that it gives desired yield considering the commercial setup. To achieve this, the study of interaction between parameters and that of parameters with yield of metals is necessary. A model has to be formulated and optimized to generate the appropriate set of input parameters values that results in maximum recovery of Zn and Mn. The lower pulp density is reason for huge quantity of media for bioleaching and it is not commercially viable so, the pulp density has to be such that the process is economical. Since, bioleaching is a natural process, which includes the utilization of the microorganisms to catalyse the oxidation.. Considering this into account, the level of pH should be such that the bio-culture is in best condition. For obtaining the optimum set of input parameters, a model has to be established which considers interaction between parameters and accurately predict the recovery of Zn and Mn. In the following, the brief details about the experiment for the measurement of data is provided.

Novel optimization method for recycling batteries

Experiments are performed to measure the extraction of Zn and Mn based on the input parameters such as energy substrates concentration (SC), incubating temperature (T), pulp density (PD) and pH control of bioleaching media (pH). Dismantling of the spent ZMBs was done manually. Dismantled products such as carbon rod, zinc rolled tins, copper caps, paper pieces and ferrous scraps were removed. The powder contains of battery experienced a mixed procedure consisted of mixing, drying, grinding by milling and sieving to obtain a mesh size of less than 200μm for bioleaching [20]. Sulfur-oxidizing bacteria (SOB) and iron-oxidizing bacteria (IOB) were used for bioleaching in the form of mixed culture. The energy substrates used were elemental sulfur and $FeSO_4$ to raise the SOB and IOB for maintenance and inoculums, respectively. The bioleaching media preparation was done by adding elemental sulfur and pyrite (1:1 in weight) into the basic medium containing $(NH_4)_2SO_4$, 2.0gL^{-1}; KH_2PO_4, 1.0gL^{-1}; $MgSO_4 \cdot 7H_2O$, 1.0gL^{-1}; $CaCl_2$, 0.25gL^{-1}; distilled water, 1000mL; natural pH 5.5. The input parameters such as SC (gL^{-1}) , pH, T (Celsius) , and PD % were varied between 24 to 40 gL^{-1} , 1.6 to 2.4, 30 to 40 Celsius, and 8 to 12% respectively. More details about the experiment can be found in [22]. Fig. 2 represents schematic of research problem statement.

3. Predictive modelling using Statistical based automated neural networks

Statistical based Automated Neural Network (SANN) is an artificial intelligence (AI) method in modelling of complex systems. A SANN model can optimize its response by adjusting its according to the feedback it receives. An industrial software named "STATISTICA 12" was used as operating environment for modelling SANN. When the network is executed, the input variable values are placed in the input units, and then the hidden and output layer units are executed progressively in their sequential order. The input layer comprises of the input parameters such as energy substrates concentration (SC), incubating temperature (T), pulp density (PD) and pH control of bioleaching media (pH). The output layer comprises of the two response variables (yield (%) of Zn and Mn).

Novel optimization method for recycling batteries

Compared to RSM, the SANN is an automated modelling process. This implies that any assumption of structure of model is not needed. Total of two sets of 29 data samples for Zn and Mn yield are used for modelling in present work. Sampling of data is done using random sampling algorithm where randomly 70% of data is considered as training set, 15% of data is for testing and remaining 15% for model validation. Trial-and-error method is applied to network settings determination. For extraction of Zn metal, Multilayer Perceptron (MLP) is set to minimum hidden units: 4 and maximum hidden units: 6, Networks to train is 2000 while networks to retain is 5, MLP activation functions used are for hidden layer is *tanh* and for output layer is logistic, Weight decay for hidden layer is set to .0001 for minimum and .001 for maximum, and fixed seed for network initialization is set to 2000. For extraction of Mn metal, Radial Basis Function (RBF) generally represented by Equation 1 is set to minimum hidden units: 4 and maximum hidden units: 16, Networks to train is 2000 while networks to retain is 5, and fixed seed for network initialization is set to 2000. The best model is selected based on the maximum training performance.. Reason for considering MLP as network type for analyzing extraction of Zn and RBF for Mn is because it was observed prediction of results were more accurate with the network type MLP compared to RBF for analyzing extraction of Zn, while for Mn better accuracy of prediction of result was given by RBF network type compared to other models.

$$\varphi(\boldsymbol{x}) = \boldsymbol{e}^{-\boldsymbol{\beta}||\boldsymbol{x}-\mu||^2} \quad \text{...Eqn.1}$$

Where,

φ is the output scalar function, x is the input data vector, μ refers to mean of the distribution, and β is reciprocal of standard deviation which controls the width of distribution.

4. Results and Discussion

4.1 SANN based Zn and Mn models

In this section, the performance of the SANN models including the statistical fit, two dimensional (parametric analysis) and three dimensional (interaction analysis) is discussed comprehensively. The input parameters and observed response is listed is Table 1 and the predicted values are listed in Table 2. The predicted value of Zn concentration is ranging from 4.7 g/L to 10.0 g/L and for Mn it is ranging from 9.20 g/L and 12.50 g/L. As been seen in table 2, the predicted and actual values for both Zn and Mn are close to each other. The best fit SANN model obtained for extraction of Zn is MLP 4-5-1 and for the extraction of Mn is RBF 4-16-1 (Table.3).

Figure 3(a) and Figure 4(a) shows the goodness-of-fit of the SANN model for Zn and Mn extraction respectively. It can be observed from the Figure 3(a) and Figure 4(a) that most data points lie near the regression line y=x, which indicates the estimated values calculated using the SANN model is close to the actual values with higher value of coefficient of determination (R^2). The smaller variation between the calculated values and the experimental values reveals that the SANN based Zn and Mn models are accurate. Which can be observed from figure 3(b) and 4(b) for there corresponding best fit model MLP 4-5-1 and RBF 4-15-1 respectively.

The coefficient of determination values for Zn and Mn are 0.941 and 0.964 respectively. While the regression line equation for Zn and Mn extraction is as follows,

$$\boldsymbol{predicted\ Zn = 0.935(Observed\ Zn) + 0.4119} \qquad \textbf{...(2)}$$

$$\boldsymbol{predicted\ Mn = 0.945(Observed\ Mn) + 0.5299} \qquad \textbf{...(3)}$$

Parametric analysis is then performed on the model to investigate the effects of each input parameters on extraction of Zn and Mn from spent ZMBs. In this analysis, one input is changing while the others are kept constant at their average values. Figure 5 shows the effects of each independent variable on the extraction of Zn and Mn. From Figure 5 (a), it can be concluded that that there’s a converse interrelation between SC and Zn extraction, The values of Zn extraction is decreasing for whole range of SC. In Figure 5 (b) for the pH range 1.6-1.9, the value of Zn extraction is increasing and from 1.9-2.4 the values of Zn extraction is found to be decreasing, The peak value of Zn extraction is found around 1.9 pH . In Figure 5 (c) for the entire range there is negative correlation between T and Zn extraction. In Figure 5 (d) the peak value of Zn extraction is obtained in range of 9.5-10% PD. It's dome like graph, for initial range from 8% to peak value, the value of Zn extraction is increasing with increasing PD, but, after that there is negative correlation between Zn extraction and PD limiting at 12%. For Mn extraction, In Figure 5 (e) the value of Mn extraction is constant for range 24-25 g/L of SC and from 24 to 40 g/L it's found to be decreasing. In Figure 5 (f), for the pH range 1.6-1.8, the value of Mn extraction is increasing and for range 1.8-2.4 it's decreasing linearly. The peak value of Mn extraction is obtained at 1.8 pH . In Figure 5 (g) the peak value of Mn extraction is obtained around 36 °C. From 30℃ to 36°C, the value of Mn extraction is increasing linearly and from 36℃ to 40℃ it's found to be decreasing. In Figure 5 (h), the value of Mn extraction is decreasing for range 8-11.5% of PD. The slope is more negative in 8-10.5% range compared to 11.0-12% range. For 11.5-12% range of PD, the values of Mn extraction is constant.

Global sensitivity analysis gives the percentage effect (%) contribution of input parameters on the two response variables. The global sensitivity analysis result for the extraction of Zn and Mn is shown in table 4.

From Table 4, we can found that that for extraction of Zn, the most contributing parameters are PD and pH while for extraction of Mn the most contributing parameters are PD and T. The effects of input parameters on the extraction of Zn and Mn are studied through the interaction analysis (3-D), In which two of the inputs are varied while others are kept constant average values. These results are in good accordance with that of the parametric analysis. Considering the global sensitivity analysis, interaction analysis is obtained only between those parameters which affect the response variable most. In Figure 6 (a) the dome structure is obtained which signifies that for pH around 1.9 and PD in range of 9.5-10% gives maximum extraction of Zn. Figure 6 (b) is corresponding contour plot of Figure 6 (a). In Figure 6 (c), curved ramp structure is obtained. For the given range of 36℃ to 38℃ and PD in range of 7.5-8%, gives maximum extraction of Mn. Figure 6 (d) is corresponding contour plot of Figure 6 (c). In Figure 6 (e), the curved ramp structure is obtained which signifies that for T at 30℃ and PD at 10% gives maximum extraction of Zn. Figure 6 (f) is corresponding contour plot of Figure 6 (e). In Figure 6 (g), the plot signifies that for PD in range 7.5-8% and for pH 2.0 the maximum extraction of Mn is obtained. Figure 6 (h) is corresponding contour plot of Figure 6 (g). It can be formulated that optimum values of input parameters for bioleaching process are SC=32 g/L, pH=1.9-2.0, T=30℃, PD=10% for Zn and SC=32 g/L, pH=2.0, T=35℃, PD=8% for Mn. Considering the initial concentration of Zn and Mn in spent ZMBs, the maximum extraction efficiencies for Zn and Mn are 50%and 50.5% respectively for the obtained SANN models.

4.2 ANOVA model for Zn and Mn extraction and comparison with SANN models

In this section, the result of ANOVA model is being discussed when applied on the data set shown in Table 1. Table 5 gives the predicted value of response from ANOVA model. Table 6 shows the Linear regression statistics. It can be observed from Table 5, the maximum output for Zn and Mn is obtained at run no. 1 and run no. 25 respectively. It can be seen from Table 6 that coefficient of determination for Zn response is lower than 0.90. This shows that linear ANOVA model is not able to approximately accurate when compared with SANN models where coefficient of determination values is found to be higher than 0.94 (Table 3). Please refer Appendix 1 for tables A1 and A2 on analysis of variance and computation of coefficient of input parameters.

Finally, the optimum parameter values for maximum recovery of Zn determined are SC=32 g/L, pH=1.9-2.0, T=30˚C, PD=10% and SC=32 g/L, pH=2.0, T=35˚C, PD=8% for maximum extraction of Mn. Considering the initial concentration of Zn and Mn in spent ZMBs, the maximum extraction efficiencies for Zn and Mn are 50%and 50.5% respectively for the obtained SANN models. Though it is less than the previously reported work where maximum extraction efficiencies for Zn and Mn are 52.5%and 52.4% respectively [20]. But, it should be noted that the method implemented in previous work [20] is more complex and doesn't effectively represent the process behaviour compared to SANN model. Xin et. al [18], reported 60% maximum extraction of Mn, but these process is very length as it takes 7 days to attain the maximum extraction of Mn.

5.Conclusions

The present study emphasizes the research issue on the evaluation and determination of optimum values of energy substrates concentration (SC), incubating temperature (T), pulp density (PD) and pH control of bioleaching media (pH) for maximum extraction of Zn and Mn from the spend ZMBs batteries. In this perspective, the paper proposes the statistical based Automated Neural Network for optimizing the settings of bioleaching process for Zn and Mn removal from spent ZMBs. Experiments were performed to validate the SANN models with 18% of the total samples used for testing and validation. It was found that the proposed SANN based metal extraction models exactly calculated the production of Zn and Mn with higher values of coefficient of determination (0.94). A comparative analysis of SANN with ANOVA shows that the latter is not able to approximately accurate with coefficient of determination values achieved as only 0.66. Based on global sensitivity analysis, it was found that for the extraction of Zn, the most contributing parameters are PD and pH while for extraction of Mn the most contributing parameters are PD and T. The optimum parameter values for maximum recovery of Zn determined are SC=32 g/L, pH=1.9-2.0, T=30˚C, PD=10% and SC=32 g/L, pH=2.0, T=35˚C, PD=8% for maximum extraction of Mn.

References

[1] Zhang, X., Li, L., Fan, E., Xue, Q., Bian, Y., Wu, F., and Chen, R., 2018, “Toward sustainable and systematic recycling of spent rechargeable batteries,” *Chemical Society Reviews*, 47(19), pp.7239-7302.

[2] Eftekhari, A., 2019, “Lithium Batteries for Electric Vehicles: From Economy to Research Strategy,” *ACS Sustainable Chemistry & Engineering*, 7(6), pp.5602-5613.

[3] Chung, D., Elgqvist, E., and Santhanagopalan, S., 2016, “Automotive lithium-ion cell manufacturing: Regional cost structures and supply chain considerations (No. NREL/TP-6A20-66086),” National Renewable Energy Lab.(NREL), Golden, CO (United States).

[4] Curry, C., 2017, “Lithium-ion battery costs and market,” *Bloomberg New Energy Finance*, 5.

[5] Huang, B., Pan, Z., Su, X., and An, L., 2018, “Recycling of lithium-ion batteries: Recent advances and perspectives,” *Journal of Power Sources*, 399, pp.274-286.

[6] Viswanathan, B., 2016, “Energy sources: fundamentals of chemical conversion processes and applications,” *Newnes*, chapter-12, pp.263-315.

[7] Winslow, K.M., Laux, S.J., and Townsend, T.G., 2018, “A review on the growing concern and potential management strategies of waste lithium-ion batteries,” *Resources, Conservation and Recycling*, 129, pp.263-277.

[8] Dehghani-Sanij, A.R., Tharumalingam, E., Dusseault, M.B., and Fraser, R., 2019, “Study of energy storage systems and environmental challenges of batteries,” *Renewable and Sustainable Energy Reviews*, 104, pp.192-208.

[9] Hung, Y.Y., Yin, L.T., Wang, J.W., Wang, C.T., Tsai, C.H., and Kuo, Y.M., 2018, “Recycling of spent nickel–cadmium battery using a thermal separation process,” *Environmental Progress & Sustainable Energy*, 37(2), pp.645-654.

[10] Qazi, S., 2016, “Standalone Photovoltaic (PV) Systems for Disaster Relief and Remote Areas,” *Elsevier*, chapter-2, pp.31-79.

[11] Lv, W., Wang, Z., Cao, H., Sun, Y., Zhang, Y., and Sun, Z., 2018, “A critical review and analysis on the recycling of spent lithium-ion batteries,” *ACS Sustainable Chemistry & Engineering*, 6(2), pp.1504-1521.

[12] Huang, K., Li, J., and Xu, Z., 2010, “Characterization and recycling of cadmium from waste nickel–cadmium batteries,” *Waste management*, 30(11), pp.2292-2298.

[13] Kim, T.H., Senanayake, G., Kang, J.G., Sohn, J.S., Rhee, K.I., Lee, S.W. and Shin, S.M., 2009, "Reductive acid leaching of spent zinc–carbon batteries and oxidative precipitation of Mn–Zn ferrite nanoparticles," *Hydrometallurgy*, 96(1-2), pp.154-158.

[14] Chen, L., Tang, X., Zhang, Y., Li, L., Zeng, Z., and Zhang, Y., 2011, "Process for the recovery of cobalt oxalate from spent lithium-ion batteries," *Hydrometallurgy*, 108(1-2), pp.80-86.

[15] Barashev, A.R., Bazhenov, O.V., and Tarasova, Y.O., 2018, "Alternative Technology of Nickel-Cadmium Batteries Recycling," *Solid State Phenomena*, 284, pp.822-827.

[16] Sayilgan, E., Kukrer, T., Civelekoglu, G., Ferella, F., Akcil, A., Veglio, F., and Kitis, M., 2009, "A review of technologies for the recovery of metals from spent alkaline and zinc–carbon batteries," *Hydrometallurgy*, 97(3-4), pp.158-166.

[17] Zeng, G., Deng, X., Luo, S., Luo, X., and Zou, J., 2012, "A copper-catalyzed bioleaching process for enhancement of cobalt dissolution from spent lithium-ion batteries," *Journal of hazardous materials*, 199, pp.164-169.

[18] Xin, B., Jiang, W., Aslam, H., Zhang, K., Liu, C., Wang, R., and Wang, Y., 2012, "Bioleaching of zinc and manganese from spent Zn–Mn batteries and mechanism exploration," *Bioresource technology*, 106, pp.147-153.

[19] Velgosová, O., Kaduková, J., Marcinčáková, R., Palfy, P., and Trpčevská, J., 2013, "Influence of H2SO4 and ferric iron on Cd bioleaching from spent Ni–Cd batteries," *Waste management*, 33(2), pp.456-461.

[20] Niu, Z., Huang, Q., Xin, B., Qi, C., Hu, J., Chen, S., and Li, Y., 2016, "Optimization of bioleaching conditions for metal removal from spent zinc-manganese batteries using response surface methodology," *Journal of Chemical Technology & Biotechnology*, 91(3), pp.608-617.

[21] Mishra, D., Kim, D.J., Ralph, D.E., Ahn, J.G., and Rhee, Y.H., 2008, "Bioleaching of metals from spent lithium ion secondary batteries using Acidithiobacillus ferrooxidans," *Waste management*, 28(2), pp.333-338.

[22] Haghshenas, D.F., Bonakdarpour, B., Alamdari, E.K., and Nasernejad, B., 2012, Optimization of physicochemical parameters for bioleaching of sphalerite by Acidithiobacillus ferrooxidans using shaking bioreactors," *Hydrometallurgy*, 111, pp.22-28.

[23] Tanong, K., Coudert, L., Chartier, M., Mercier, G., and Blais, J.F., 2017, "Study of the factors influencing the metals solubilisation from a mixture of waste batteries by response surface methodology," *Environmental technology*, 38(24), pp.3167-3179.

[24] Desai, K.M., Survase, S.A., Saudagar, P.S., Lele, S.S., and Singhal, R.S., 2008, "Comparison of artificial neural network (ANN) and response surface methodology (RSM) in fermentation media optimization: case study of fermentative production of scleroglucan," *Biochemical Engineering Journal*, 41(3), pp.266-273.

[25] Ebrahimzade, H., Khayati, G.R., and Schaffie, M., 2018, "A novel predictive model for estimation of cobalt leaching from waste Li-ion batteries: Application of genetic programming for design," *Journal of environmental chemical engineering*, 6(4), pp.3999-4007.

[26] Ebrahimzade, H., Khayati, G.R., and Schaffie, M., 2019, "PSO–ANN-based prediction of cobalt leaching rate from waste lithium-ion batteries," *Journal of Material Cycles and Waste Management*, pp.1-12.

[27] Yun, L., Goyal, A., Singh, V.P., Gao, L., Peng, X., Niu, X., Wang, C.T., and Garg, A., 2019, "Experimental coupled predictive modelling based recycling of waste printed circuit boards for maximum extraction of copper," *Journal of cleaner production*, 218, pp.763-771.

[28] Novák, D., and Lehký, D., 2006, "ANN inverse analysis based on stochastic small-sample training set simulation," *Engineering Applications of Artificial Intelligence*, 19(7), pp.731-740.

[29] Ruhatiya, C., Singh, S., Goyal, A., Niu, X., Nguyen, H., Ngoc, T., Nguyen, V.H., Tran, V.M., Phung, L.E., Loan, M., and Garg, A., 2020, "Electrochemical performance enhancement of sodium-ion batteries fabricated with NaNi1/3Mn1/3Co1/3O2 cathodes using support vector regression-simplex

algorithm approach," *Journal of Electrochemical Energy Conversion and Storage*, 17(1), pp.011009, https://doi.org/10.1115/1.4044358

[30] Jiang, D., Wu, K., Chen, D., Tu, G., Zhou, T., Garg, A., and Gao, L., 2020, "A probability and integrated learning based classification algorithm for high-level human emotion recognition problems," *Measurement*, 150, pp.107049, https://doi.org/10.1016/j.measurement.2019.107049

[31] Li, W., Peng, X., Xiao, M., Garg, A., and Gao, L., 2019, "Multi-objective design optimization for mini-channel cooling battery thermal management system in an electric vehicle , *International Journal of Energy Research*, 43, pp.3668-3680, https://doi.org/10.1002/er.4518

[32] Li, W., Chen, S., Peng, X., Xiao, M., Gao, L., Garg, A., and Bao, N., 2019, "A Comprehensive Approach for the Clustering of Similar-Performance Cells for the Design of a Lithium-Ion Battery Module for Electric Vehicles," *Engineering*, 5(4), pp.795-802, https://doi.org/10.1016/j.eng.2019.07.005

[33] Goyal, A., Niu, X., Le, N.P.P., Le Huynh, N.T., Le, M.L.P., Gao, L., and Garg, A., 2019, "Precision Manufacturing of NaNi 1/3 Mn 1/3 Co 1/3 O 2 Cathodes: Study of Structure Evolution and Performance at Varied Calcination Temperatures," *Journal of Electronic Materials*, 48(8), pp.5301-5309, https://doi.org/10.1007/s11664-019-07340-1

Tables:

Table 1. Input parameters and observed response for Zn and Mn recovery during bioleaching of spent. ZMBs.

Run no.	SC g/L	pH	T (ºC)	PD%	Observed Zn g/L	Observed Mn g/L
1	28	1.8	32.5	9	9.4	11.4
2	36	1.8	32.5	9	9.1	10.9
3	28	2.2	32.5	9	7.9	10.7
4	36	2.2	32.5	9	6.4	10.6
5	28	1.8	37.5	9	8.2	11.6

6	36	1.8	37.5	9	7.8	11.5
7	28	2.2	37.5	9	6.3	11
8	36	2.2	37.5	9	5.4	11
9	28	1.8	32.5	11	9.1	10
10	36	1.8	32.5	11	8.7	9.7
11	28	2.2	32.5	11	6.6	9.7
12	36	2.2	32.5	11	6	9.3
13	28	1.8	37.5	11	5.8	10.2
14	36	1.8	37.5	11	5.5	10
15	28	2.2	37.5	11	5.6	9.3
16	36	2.2	37.5	11	5.3	9.1
17	32	2	35	10	9.8	10.7
18	32	2	35	10	9.8	10.5
19	24	2	35	10	10.3	10.8
20	40	2	35	10	7.2	10.1
21	32	1.6	35	10	7.3	10.5
22	32	2.4	35	10	4.8	9.8
23	32	2	30	10	8.6	9.5
24	32	2	40	10	6.4	9.7
25	32	2	35	8	6.6	12.5
26	32	2	35	12	4.6	9.7
27	32	2	35	10	9.8	11
28	32	2	35	10	9.8	10.5
29	32	2	35	10	9.9	10.8

Table 2. Predicted response from SANN based Zn and Mn models

Run no.	Observed Zn g/L	Predicted Zn g/L	Observed Mn g/L	Predicted Mn g/L
1	9.4	9.1	11.4	10.9
2	9.1	8.3	10.9	10.9
3	7.9	7.5	10.7	10.7
4	6.4	5.9	10.6	10.5
5	8.2	8.1	11.6	11.5
6	7.8	7.7	11.5	11.5
7	6.3	6.2	11	11.0
8	5.4	4.9	11	10.9
9	9.1	8.5	10	9.9
10	8.7	8.4	9.7	9.6
11	6.6	7	9.7	9.6
12	6	6	9.3	9.3
13	5.8	5.5	10.2	10.2
14	5.5	5.1	10	9.9
15	5.6	5.9	9.3	9.3
16	5.3	5.7	9.1	9.2
17	9.8	9.5	10.7	10.6
18	9.8	9.5	10.5	10.6
19	10.3	10.0	10.8	10.8

20	7.2	7.4	10.1	10.1
21	7.3	7.5	10.5	10.5
22	4.8	4.7	9.8	9.8
23	8.6	10.1	9.5	9.6
24	6.4	6.8	9.7	9.7
25	6.6	6.6	12.5	12.5
26	4.6	4.9	9.7	9.7
27	9.8	9.5	11	10.6
28	9.8	9.5	10.5	10.6
29	9.9	9.5	10.8	10.6

Table 3. Best fit SANN model for extraction of Zn and Mn.

Metal (Response)	Net. name	Training perf.	Test perf.	Validation perf	Training error	Test error	Validation error	Training algorithm	Hidden activation	Output activation
Zn	MLP 4-5-1	0.984017	0.931815	0.998092	0.059620	0.315376	0.052295	BFGS 51	Tanh	Logistic
Mn	RBF 4-16-1	0.997045	0.988236	0.99909	0.001713	0.011013	0.057928	RBFT	Gaussian	Identity

Table 4. Global sensitivity analysis showing percentage contribution of inputs on the extraction of Zn and Mn

Metal (Response)	Network	PD %	T ˚C	pH	SC g/L
Zn	MLP 4-5-1	11.7	5.6	10.1	2.5
Mn	RBF 4-16-1	21.0	6.5	4.1	1.6

Table 5. Predicted response of linear ANOVA model and observed responses (Zn and Mn extraction)

Run no.	Observed Zn g/L	Predicted Zn g/L	Observed Mn g/L	Predicted Mn g/L
1	9.4	10.0	11.4	11.4
2	9.1	9.10	10.9	11.2
3	7.9	8.4	10.7	10.9
4	6.4	7.5	10.6	10.7
5	8.2	8.5	11.6	11.6
6	7.8	7.6	11.5	11.3
7	6.3	6.9	11	11.1
8	5.4	6.0	11	10.8
9	9.1	9.0	10	10.0
10	8.7	8.1	9.7	9.7
11	6.6	7.4	9.7	9.5
12	6	6.5	9.3	9.3
13	5.8	7.5	10.2	10.2
14	5.5	6.6	10	9.9
15	5.6	5.9	9.3	9.7
16	5.3	5.0	9.1	9.4
17	9.8	7.5	10.7	10.4
18	9.8	7.5	10.5	10.4
19	10.3	8.4	10.8	10.7
20	7.2	6.6	10.1	10.2
21	7.3	9.1	10.5	10.9
22	4.8	5.9	9.8	9.9
23	8.6	9.0	9.5	10.3
24	6.4	6.0	9.7	10.6
25	6.6	8.5	12.5	11.8
26	4.6	6.5	9.7	9
27	9.8	7.5	11	10.4
28	9.8	7.5	10.5	10.4
29	9.9	7.5	10.8	10.4

Table 6. Regression statistics for ANOVA model for Zn and Mn extraction

	Response Zn	**Response Mn**
Multiple R	0.64	0.89
R square	0.42	0.80
Adjusted R square	0.33	0.77
Standard Error	1.45	0.38
Observations	29	29

Figures uploaded as (tiff file):

1. **Figure 1. Bioleaching process and its optimization.**

2. **Figure 2. Schematic of research problem statement.**

3. **Figure 3(a). Coefficient of determination for SANN based Zn model**

4. **Figure 3(b). Zn extraction vs Run no. for MLP 4-5-1 model.**

5. **Figure 4(a). Coefficient of determination for SANN based Mn model.**

6. **Figure 4(b). Mn extraction vs Run no. for RBF 4-16-1 model.**

7. **Figure 5(a, b,c d, e, f, g, h). 2D plots showing the effects of one inputs on the extraction of Zn and Mn.**

8. **Figure 6(a, b, c, d, e, f, g, h). 3D plots and corresponding contour plots showing the interaction effects of the inputs on the extraction of Zn and Mn.**

APPENDIX 1

Table A1. Analysis of Variance (ANOVA) for Zn and Mn extraction

Response		df	SS	MS	F
Zn	Regression	4	39.37038333	9.842595833	4.616183808
	Residual	24	51.17263736	2.132193223	-
	Total	28	90.54302069	-	-
Mn	Regression	4	14.18423333	3.546058333	24.11760483
	Residual	24	3.528766667	0.147031944	-
	Total	28	17.713	-	-

Table A2. Values of regression coefficients for Zn/Mn extraction

Response		Coefficients	Standard error
Zn	Intercept	34.52106322	6.398481123
	SC	-0.1128125	0.07451568
	Ph	-3.960416667	1.490313594
	T	-0.298166667	0.119225087
	PD	-0.50375	0.298062719
Mn	Intercept	20.10833333	1.680232822
	SC	-0.033125	0.019567721
	Ph	-1.245833333	0.391354412
	T	0.028	0.031308353
	PD	-0.711666667	0.078270882

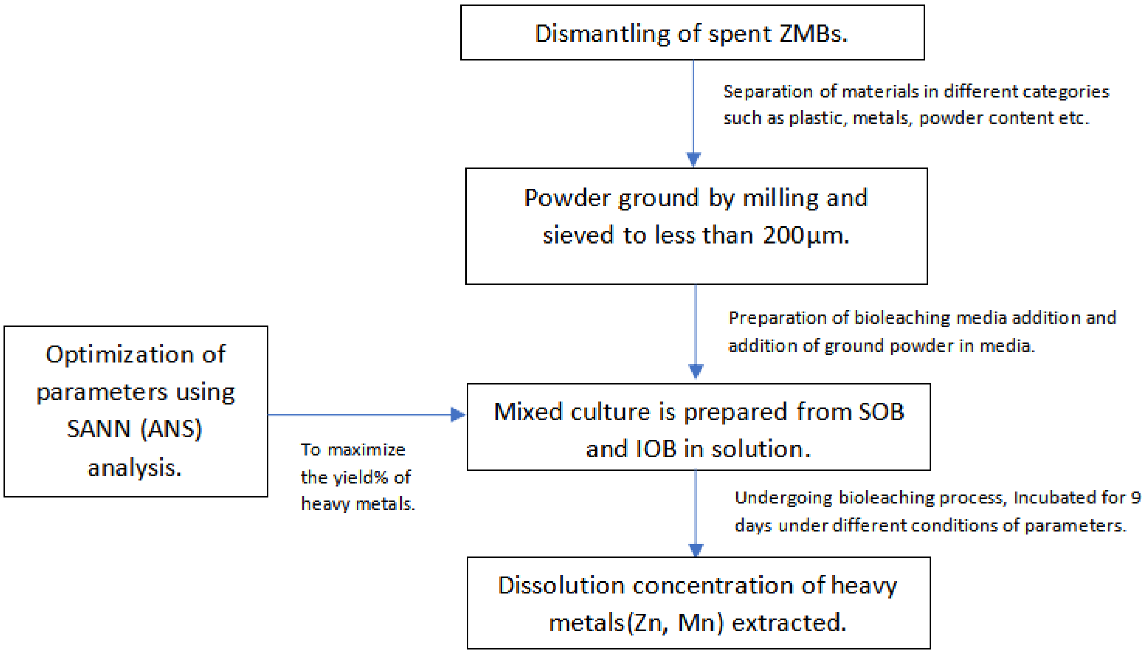
Dismantling of spent ZMBs.
Separation of materials in different categories such as plastic, metals, powder content etc.
Powder ground by milling and sieved to less than 200µm.
Preparation of bioleaching media addition and addition of ground powder in media.
Optimization of parameters using SANN (ANS) analysis.
To maximize the yield% of heavy metals.
Mixed culture is prepared from SOB and IOB in solution.
Undergoing bioleaching process, Incubated for 9 days under different conditions of parameters.
Dissolution concentration of heavy metals(Zn, Mn) extracted.

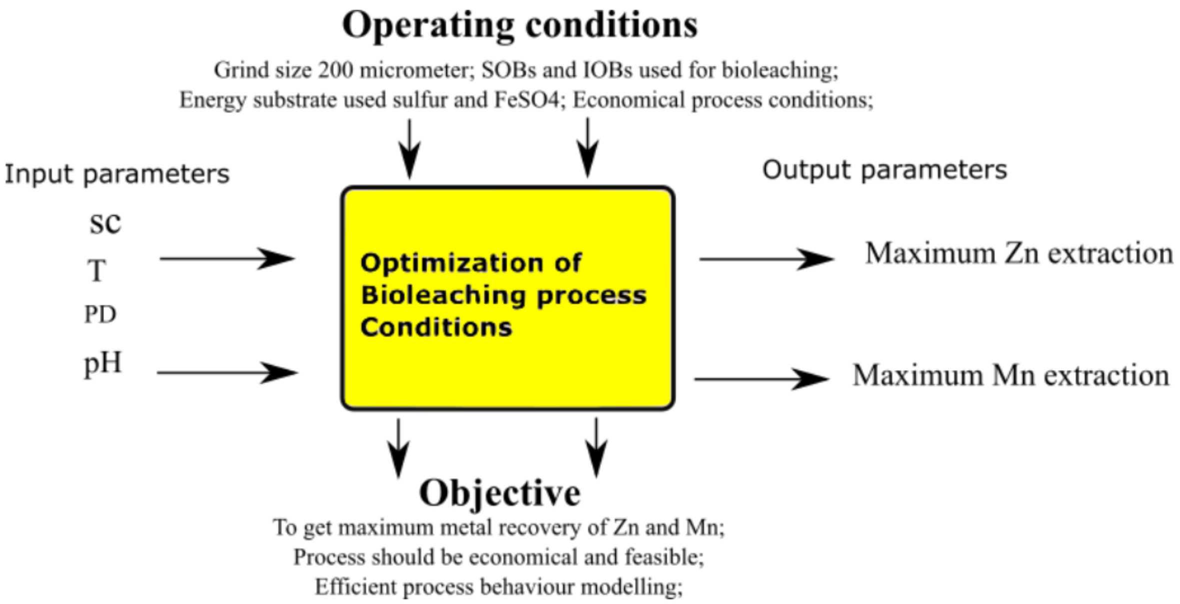
Operating conditions
Grind size 200 micrometer; SOBs and IOBs used for bioleaching;
Energy substrate used sulfur and FeSO4; Economical process conditions;
Input parameters
SC
T
PD
pH
Optimization of Bioleaching process Conditions
Output parameters
Maximum Zn extraction
Maximum Mn extraction
Objective
To get maximum metal recovery of Zn and Mn;
Process should be economical and feasible;
Efficient process behaviour modelling;

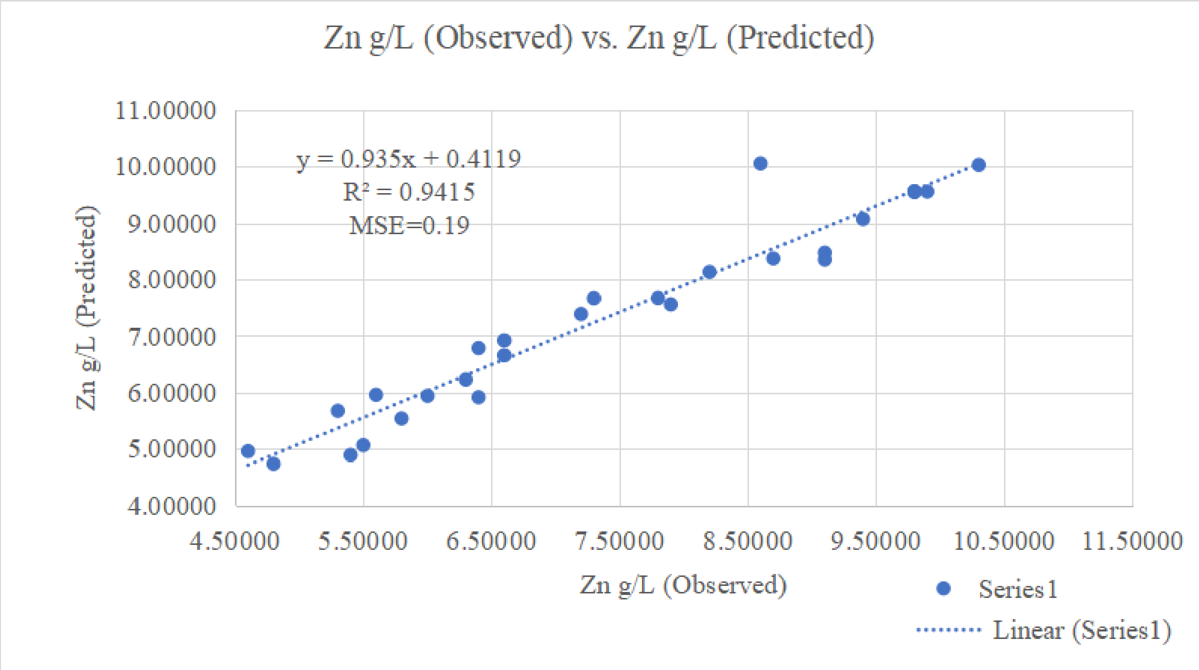
Zn g/L (Observed) vs. Zn g/L (Predicted)
y = 0.935x + 0.4119
R² = 0.9415
MSE=0.19
Zn g/L (Predicted)
Zn g/L (Observed)
11.00000
10.00000
9.00000
8.00000
7.00000
6.00000
5.00000
4.00000
4.50000
5.50000
6.50000
7.50000
8.50000
9.50000
10.50000
11.50000
Series1
Linear (Series1)

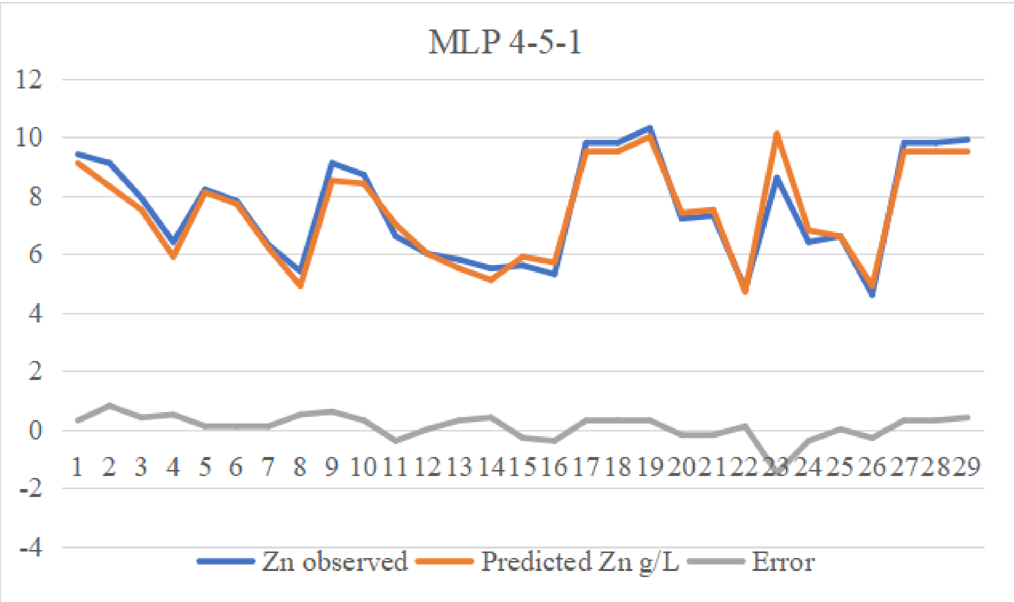
MLP 4-5-1
12
10
8
6
4
2
0
-2
-4
1 2 3 4 5 6 7 8 9 10 11 12 13 14 15 16 17 18 19 20 21 22 23 24 25 26 27 28 29
Zn observed
Predicted Zn g/L
Error

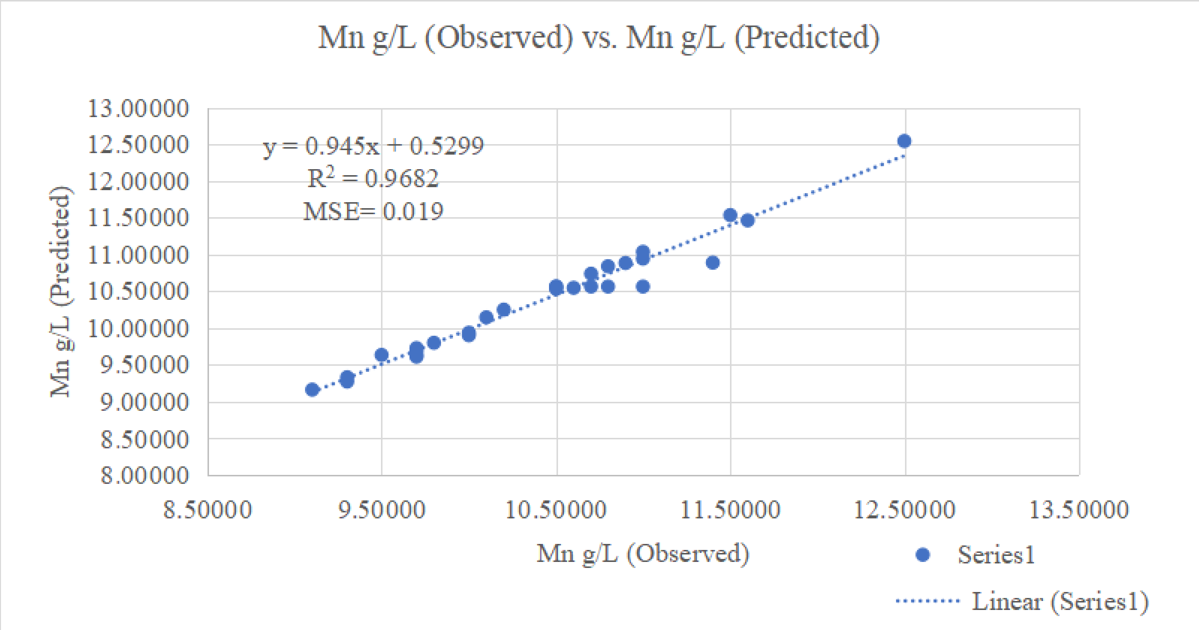

Mn g/L (Observed) vs. Mn g/L (Predicted)
y = 0.945x + 0.5299
R^2 = 0.9682
MSE= 0.019
13.00000
12.50000
12.00000
11.50000
11.00000
10.50000
10.00000
9.50000
9.00000
8.50000
8.00000
Mn g/L (Predicted)
8.50000
9.50000
10.50000
11.50000
12.50000
13.50000
Mn g/L (Observed)
Series1
Linear (Series1)

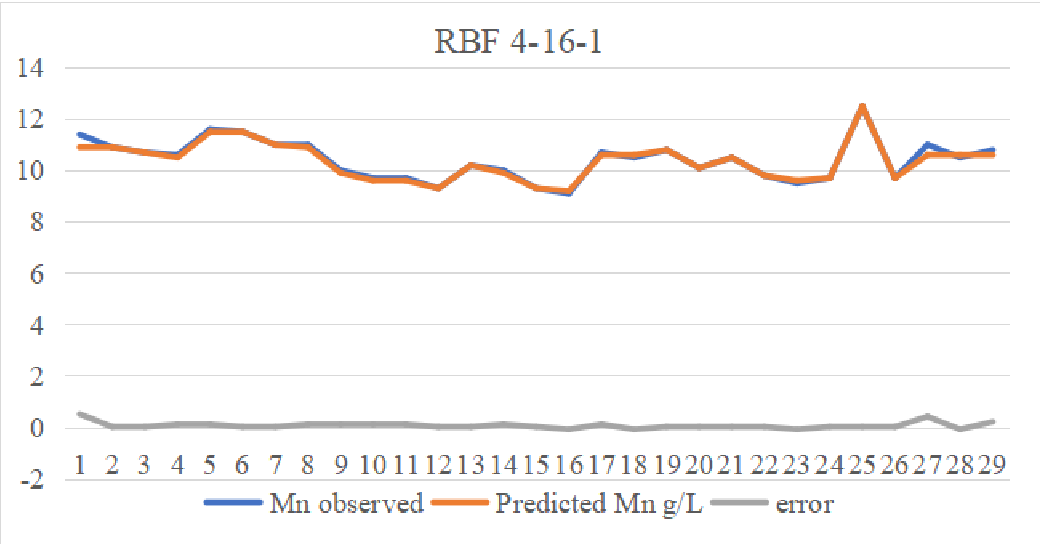

RBF 4-16-1
14
12
10
8
6
4
2
0
-2
1 2 3 4 5 6 7 8 9 10 11 12 13 14 15 16 17 18 19 20 21 22 23 24 25 26 27 28 29
Mn observed
Predicted Mn g/L
error

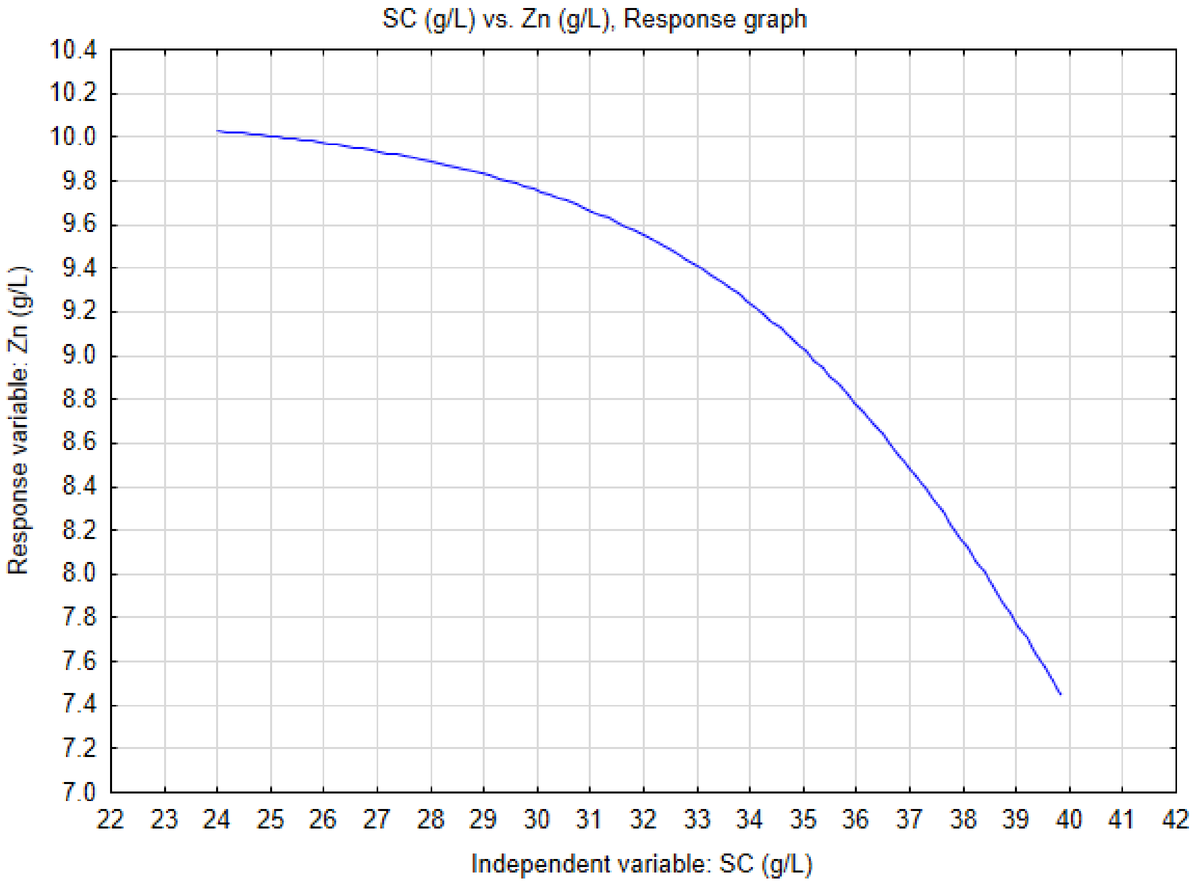
SC (g/L) vs. Zn (g/L), Response graph
Response variable: Zn (g/L)
Independent variable: SC (g/L)
10.4
10.2
10.0
9.8
9.6
9.4
9.2
9.0
8.8
8.6
8.4
8.2
8.0
7.8
7.6
7.4
7.2
7.0
22 23 24 25 26 27 28 29 30 31 32 33 34 35 36 37 38 39 40 41 42

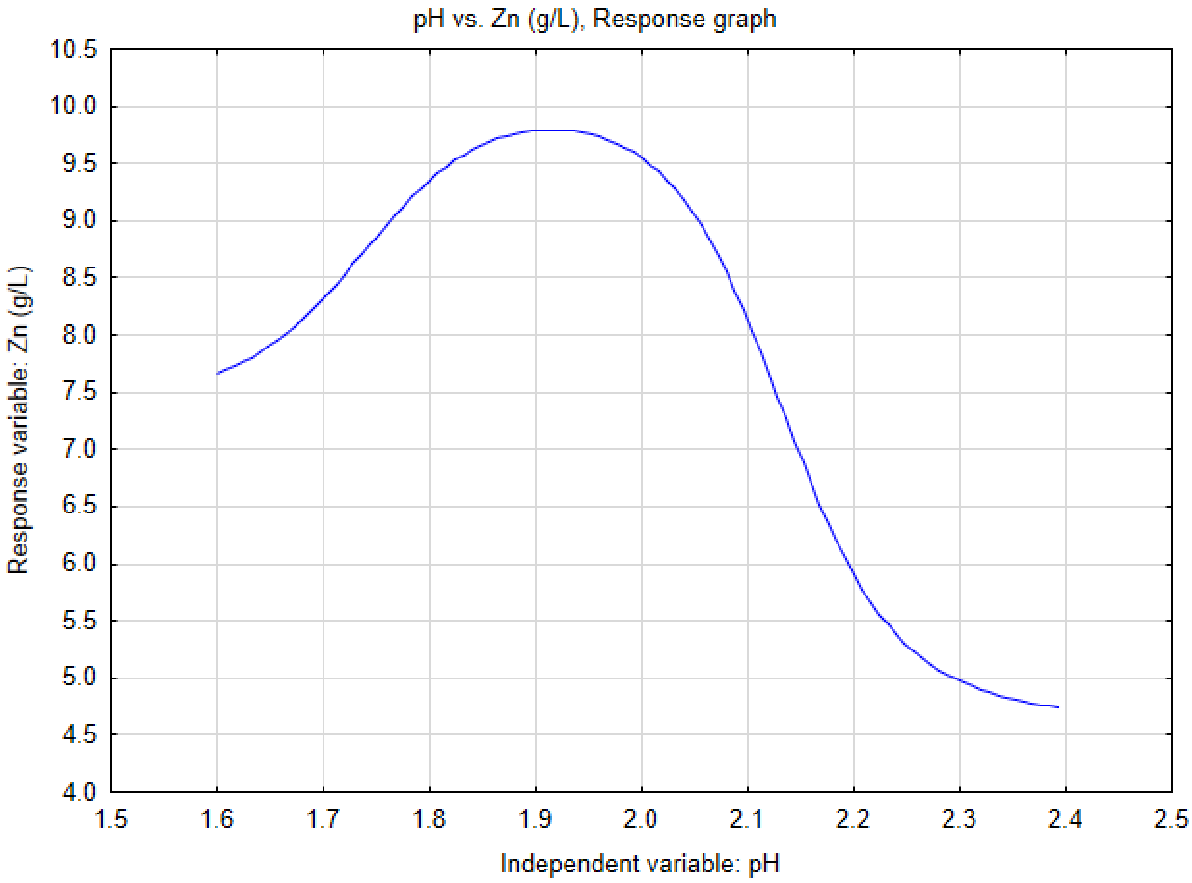
pH vs. Zn (g/L), Response graph
Response variable: Zn (g/L)
Independent variable: pH
10.5
10.0
9.5
9.0
8.5
8.0
7.5
7.0
6.5
6.0
5.5
5.0
4.5
4.0
1.5
1.6
1.7
1.8
1.9
2.0
2.1
2.2
2.3
2.4
2.5

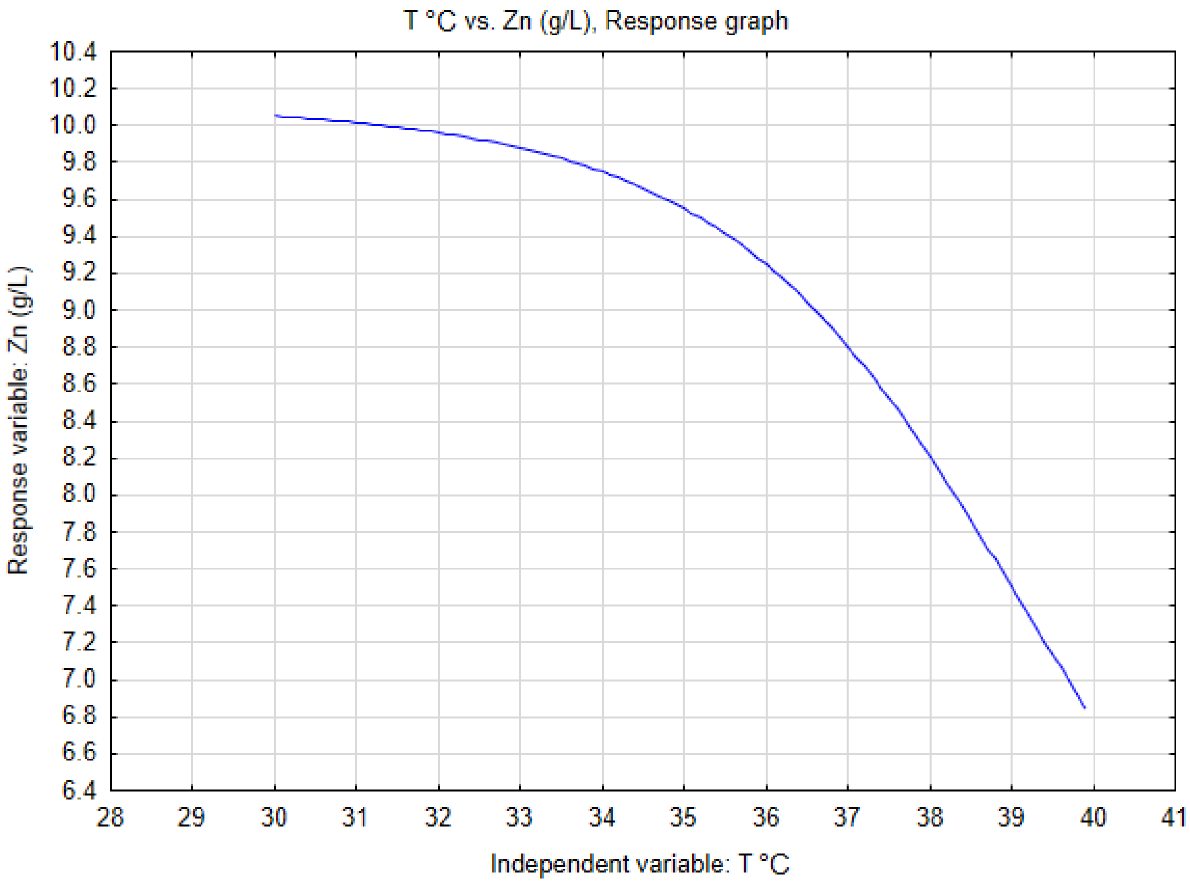
T °C vs. Zn (g/L), Response graph
Response variable: Zn (g/L)
Independent variable: T °C
10.4
10.2
10.0
9.8
9.6
9.4
9.2
9.0
8.8
8.6
8.4
8.2
8.0
7.8
7.6
7.4
7.2
7.0
6.8
6.6
6.4
28
29
30
31
32
33
34
35
36
37
38
39
40
41

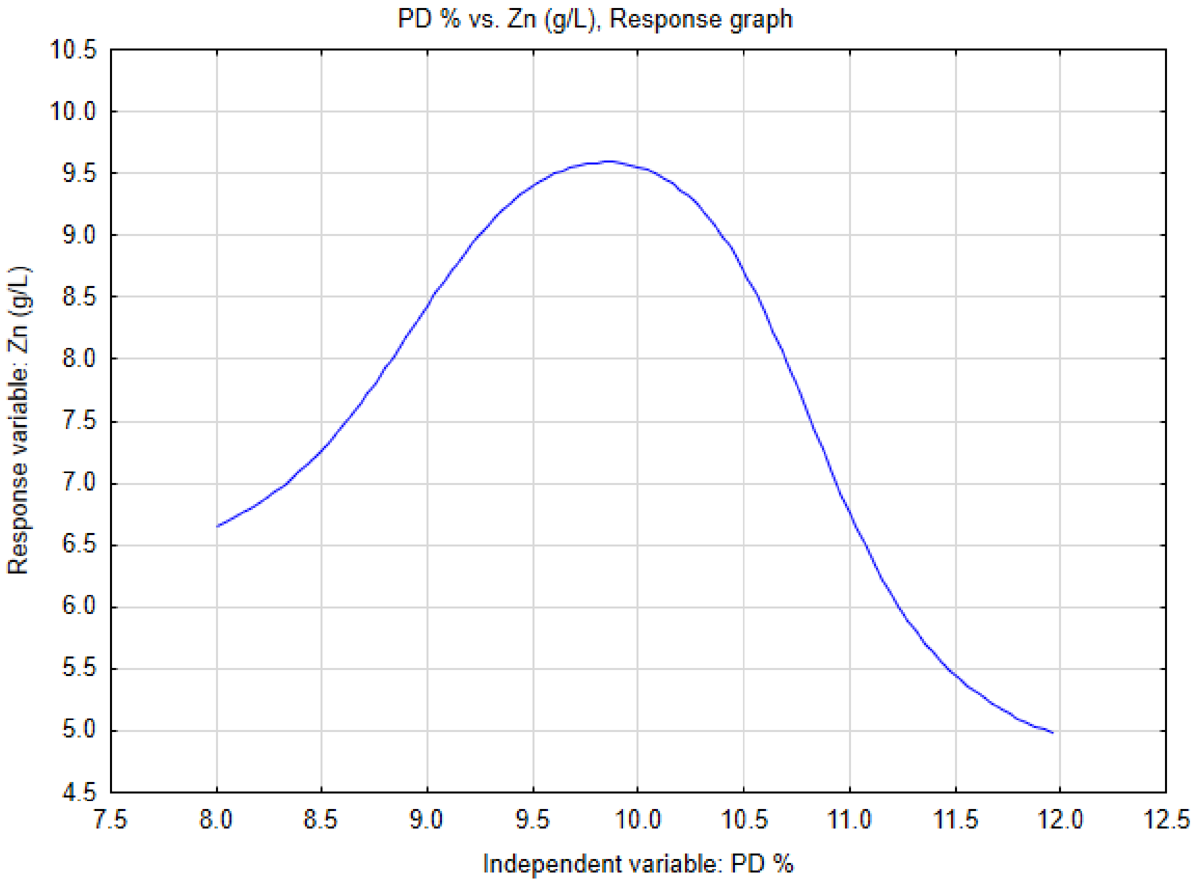
PD % vs. Zn (g/L), Response graph
Response variable: Zn (g/L)
Independent variable: PD %
10.5
10.0
9.5
9.0
8.5
8.0
7.5
7.0
6.5
6.0
5.5
5.0
4.5
7.5
8.0
8.5
9.0
9.5
10.0
10.5
11.0
11.5
12.0
12.5

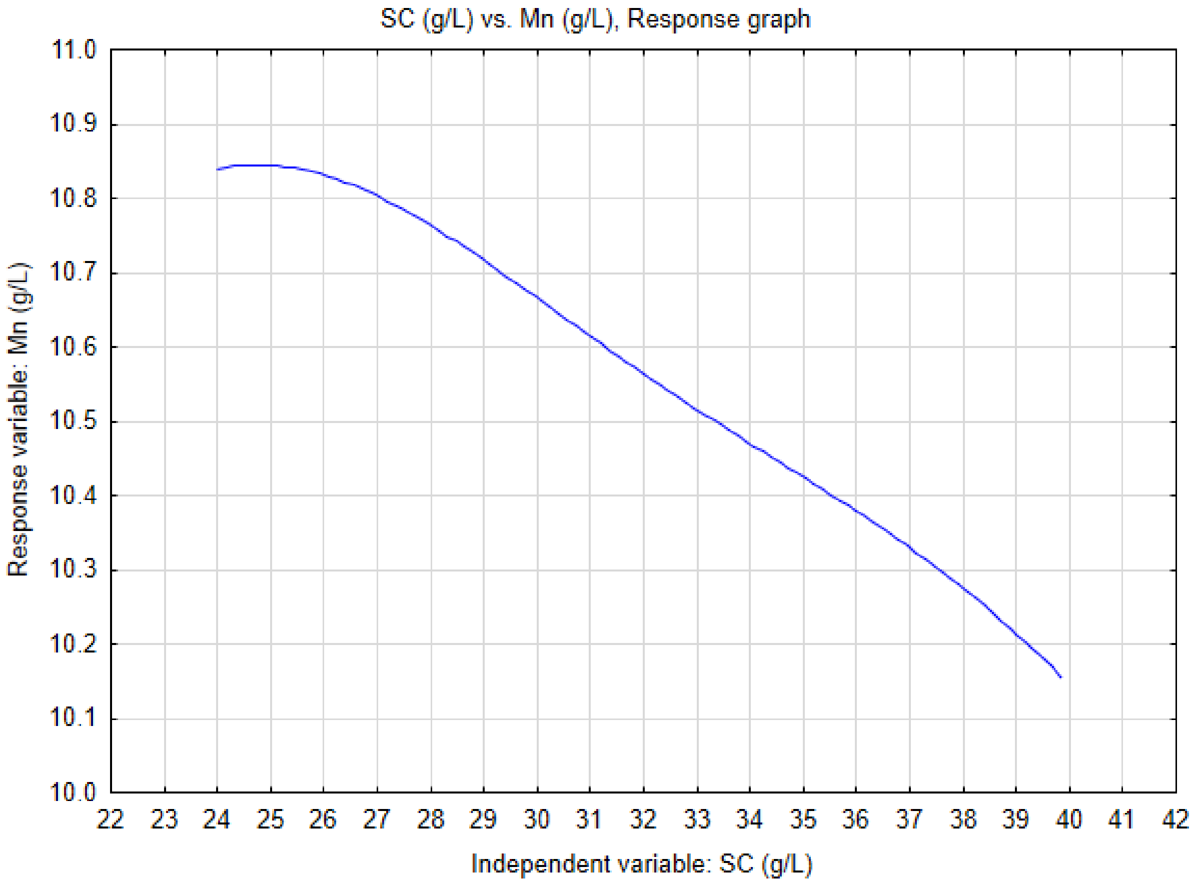
SC (g/L) vs. Mn (g/L), Response graph
Response variable: Mn (g/L)
Independent variable: SC (g/L)
11.0
10.9
10.8
10.7
10.6
10.5
10.4
10.3
10.2
10.1
10.0
22 23 24 25 26 27 28 29 30 31 32 33 34 35 36 37 38 39 40 41 42

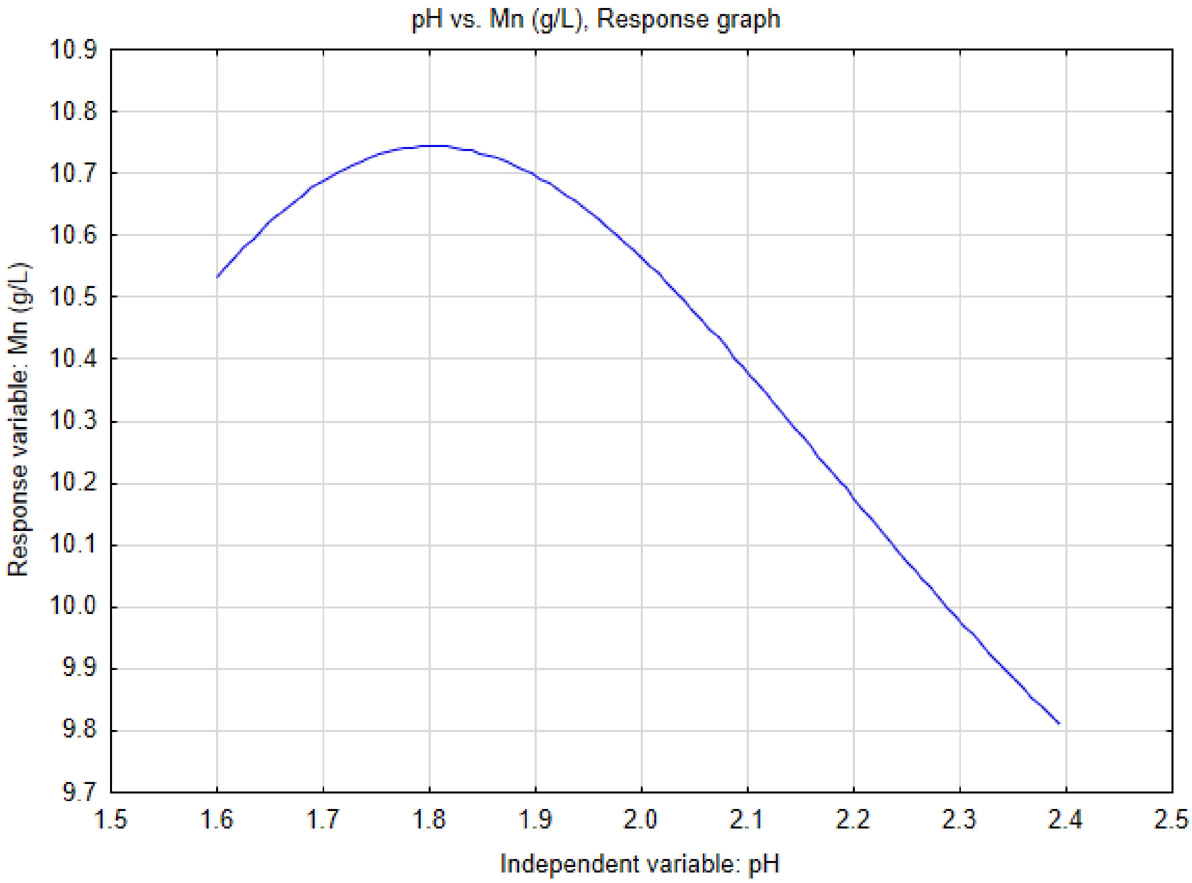
pH vs. Mn (g/L), Response graph
Response variable: Mn (g/L)
Independent variable: pH
10.9
10.8
10.7
10.6
10.5
10.4
10.3
10.2
10.1
10.0
9.9
9.8
9.7
1.5
1.6
1.7
1.8
1.9
2.0
2.1
2.2
2.3
2.4
2.5

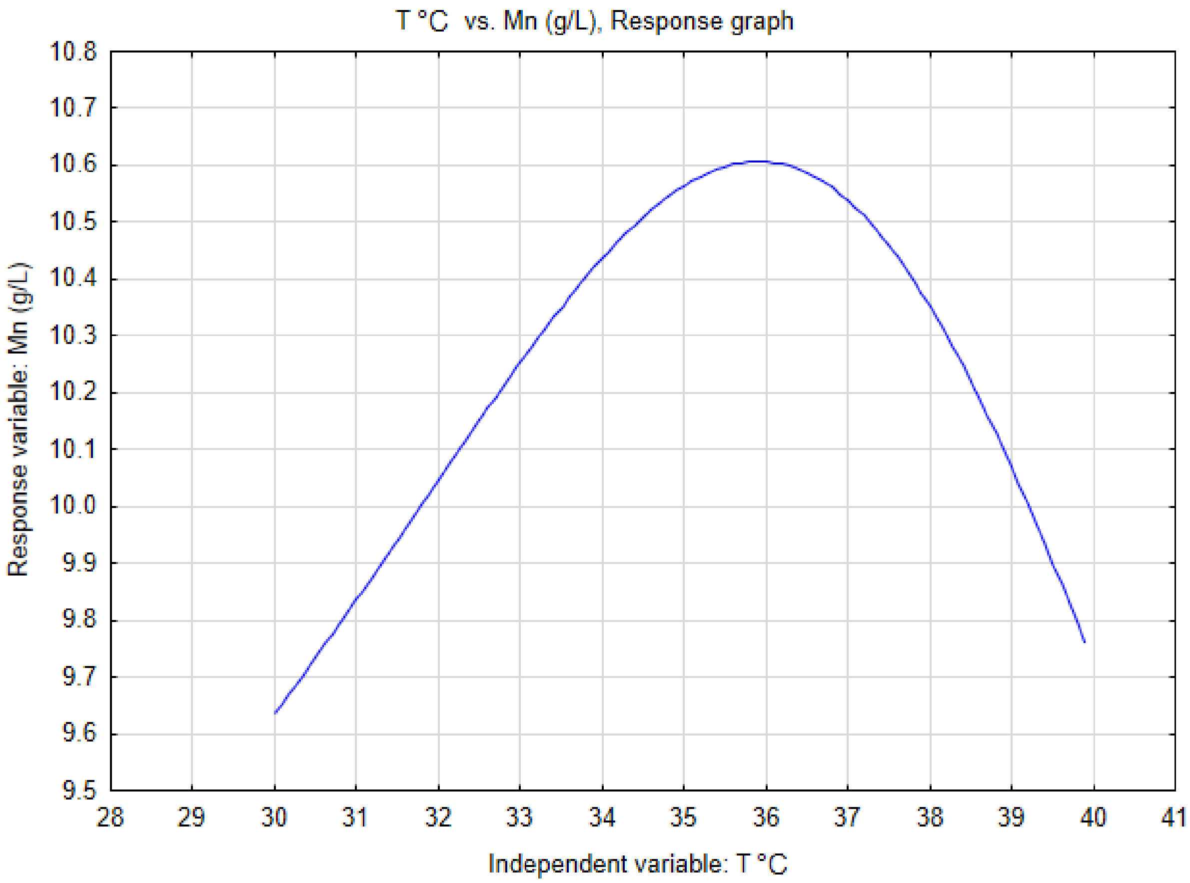
T °C vs. Mn (g/L), Response graph
Response variable: Mn (g/L)
Independent variable: T °C
10.8
10.7
10.6
10.5
10.4
10.3
10.2
10.1
10.0
9.9
9.8
9.7
9.6
9.5
28
29
30
31
32
33
34
35
36
37
38
39
40
41

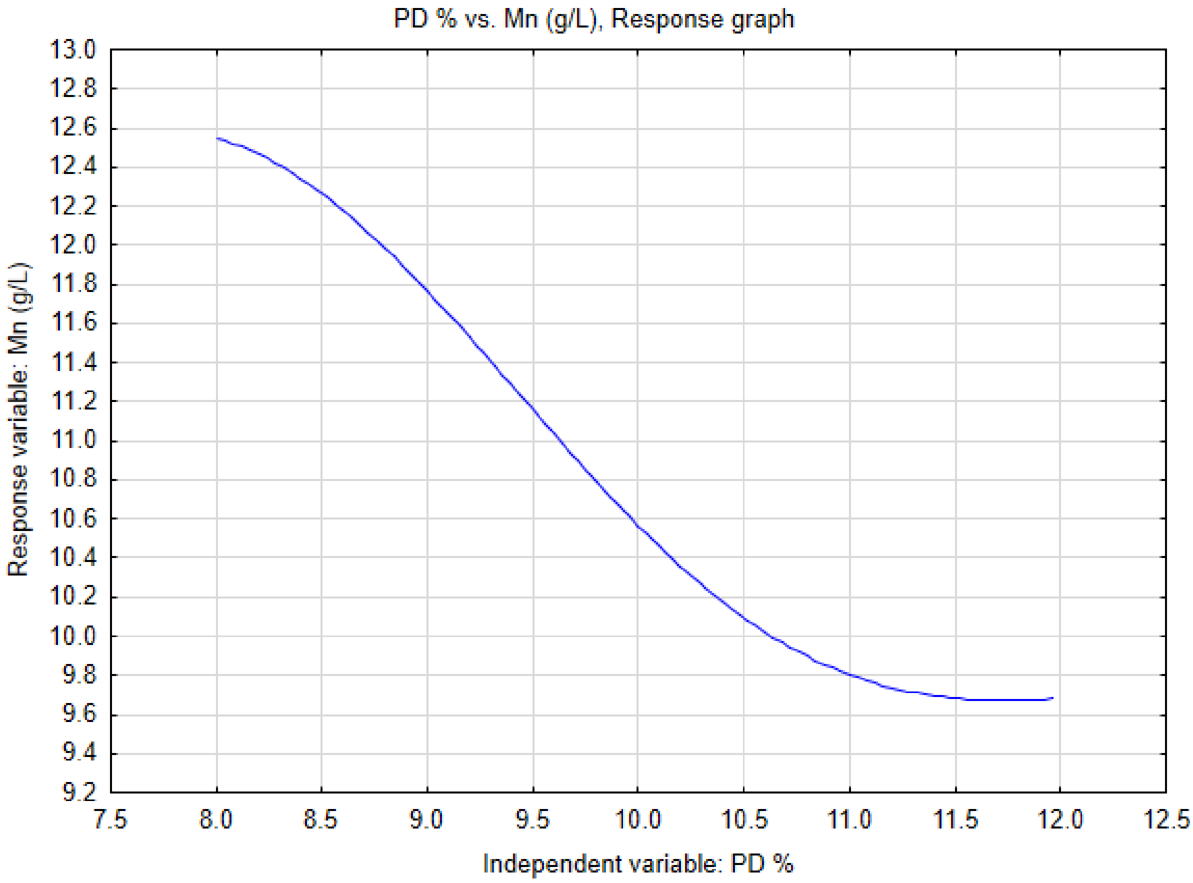
PD % vs. Mn (g/L), Response graph
Response variable: Mn (g/L)
Independent variable: PD %
13.0
12.8
12.6
12.4
12.2
12.0
11.8
11.6
11.4
11.2
11.0
10.8
10.6
10.4
10.2
10.0
9.8
9.6
9.4
9.2
7.5
8.0
8.5
9.0
9.5
10.0
10.5
11.0
11.5
12.0
12.5

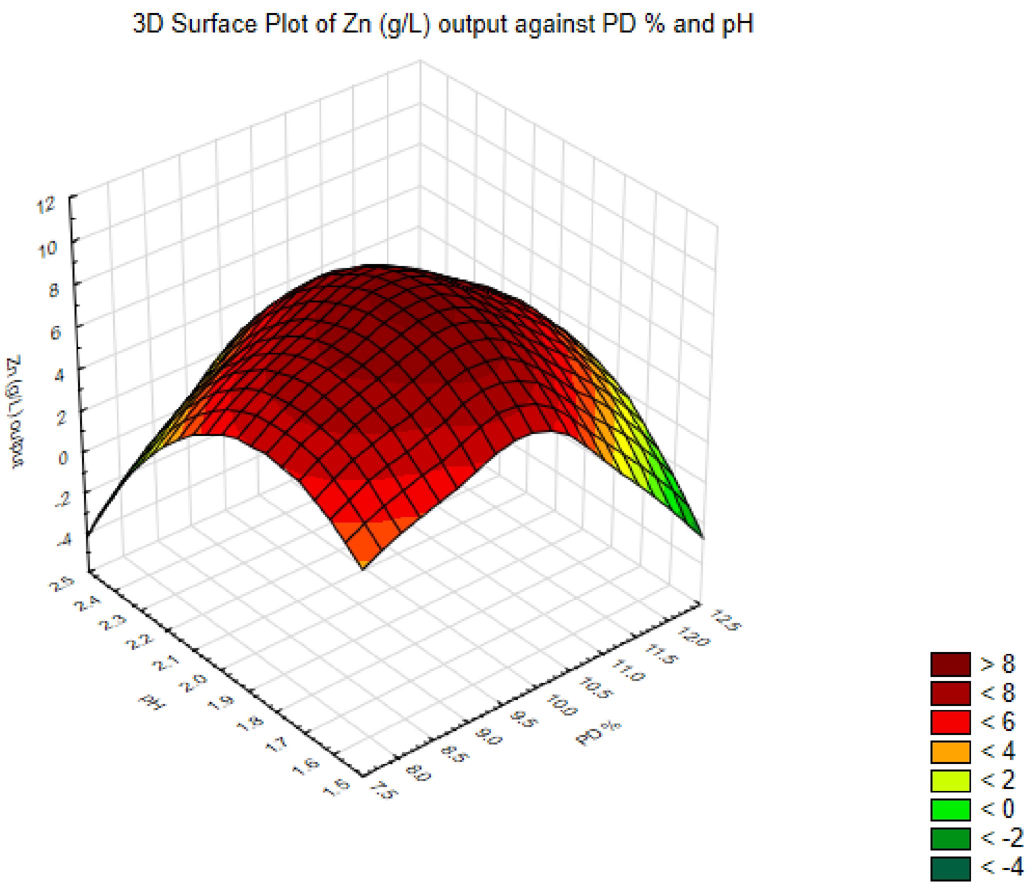
3D Surface Plot of Zn (g/L) output against PD % and pH
Zn (g/L) output
pH
PD %
> 8
< 8
< 6
< 4
< 2
< 0
< -2
< -4

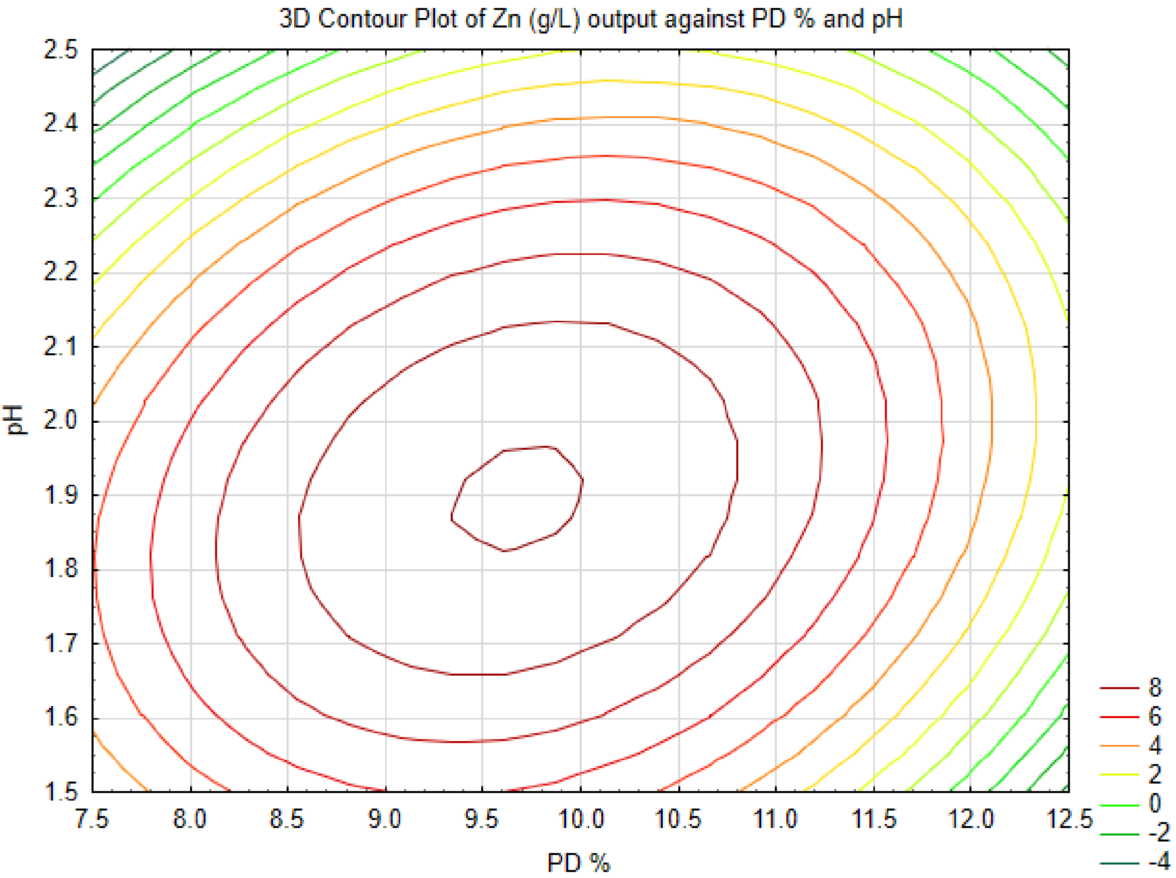
3D Contour Plot of Zn (g/L) output against PD % and pH
pH
2.5
2.4
2.3
2.2
2.1
2.0
1.9
1.8
1.7
1.6
1.5
7.5
8.0
8.5
9.0
9.5
10.0
10.5
11.0
11.5
12.0
12.5
PD %
8
6
4
2
0
-2
-4

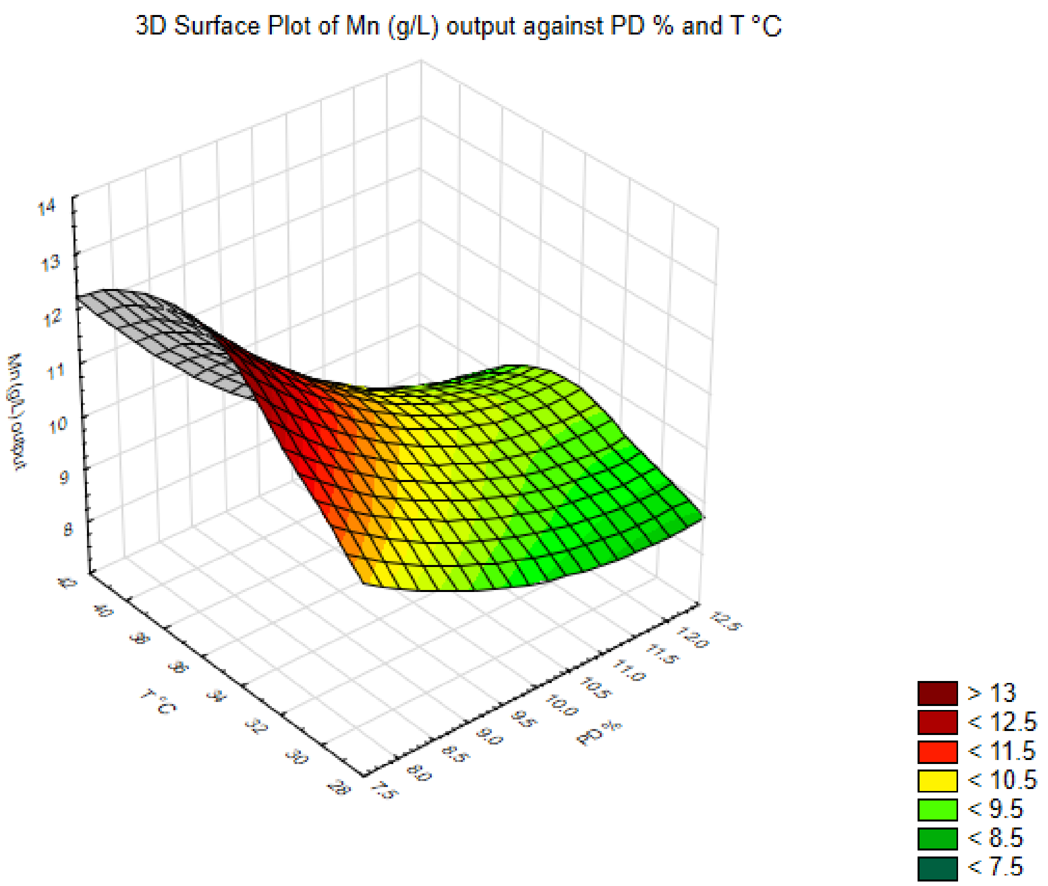
3D Surface Plot of Mn (g/L) output against PD % and T °C
Mn (g/L) output
14
13
12
11
10
9
8
T °C
42
40
38
36
34
32
30
28
PD %
7.5
8.0
8.5
9.0
9.5
10.0
10.5
11.0
11.5
12.0
12.5
> 13
< 12.5
< 11.5
< 10.5
< 9.5
< 8.5
< 7.5

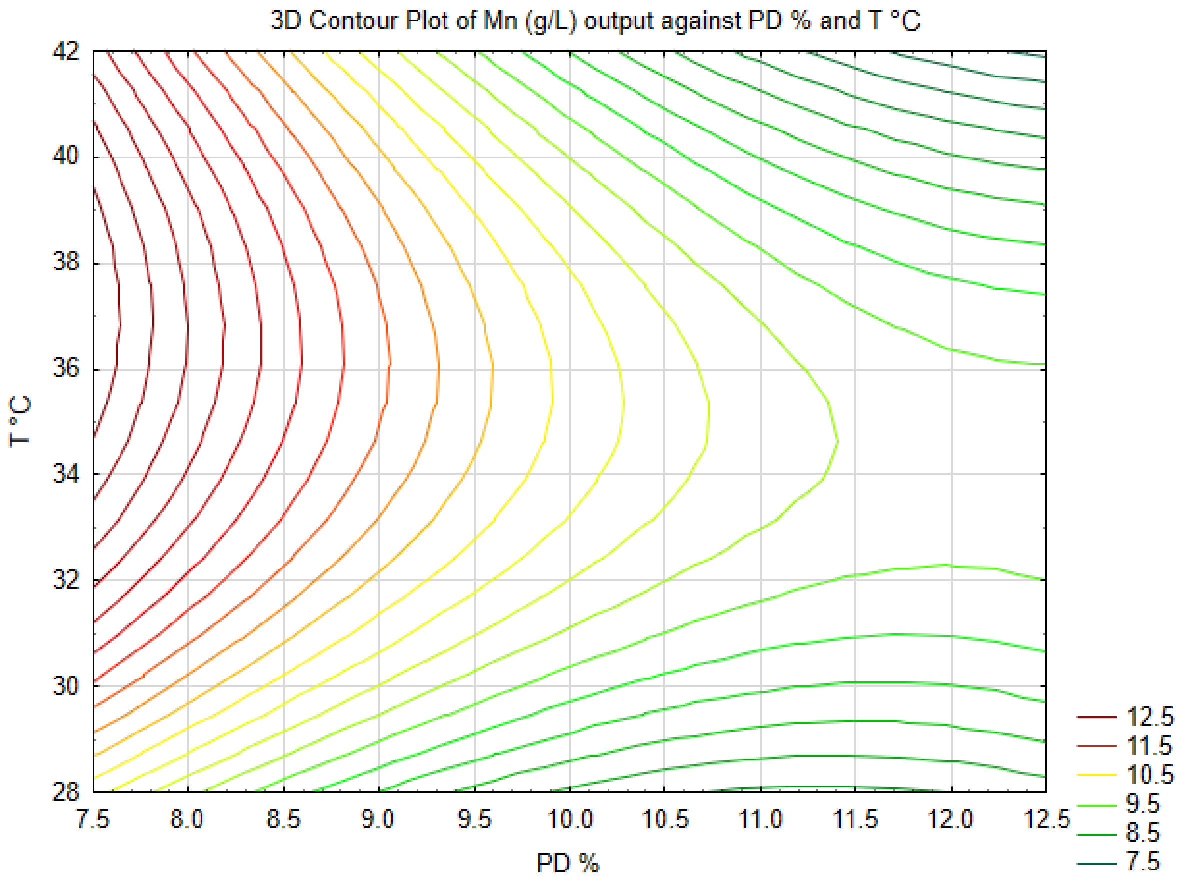
3D Contour Plot of Mn (g/L) output against PD % and T °C
42
40
38
36
34
32
30
28
T °C
7.5
8.0
8.5
9.0
9.5
10.0
10.5
11.0
11.5
12.0
12.5
PD %
12.5
11.5
10.5
9.5
8.5
7.5

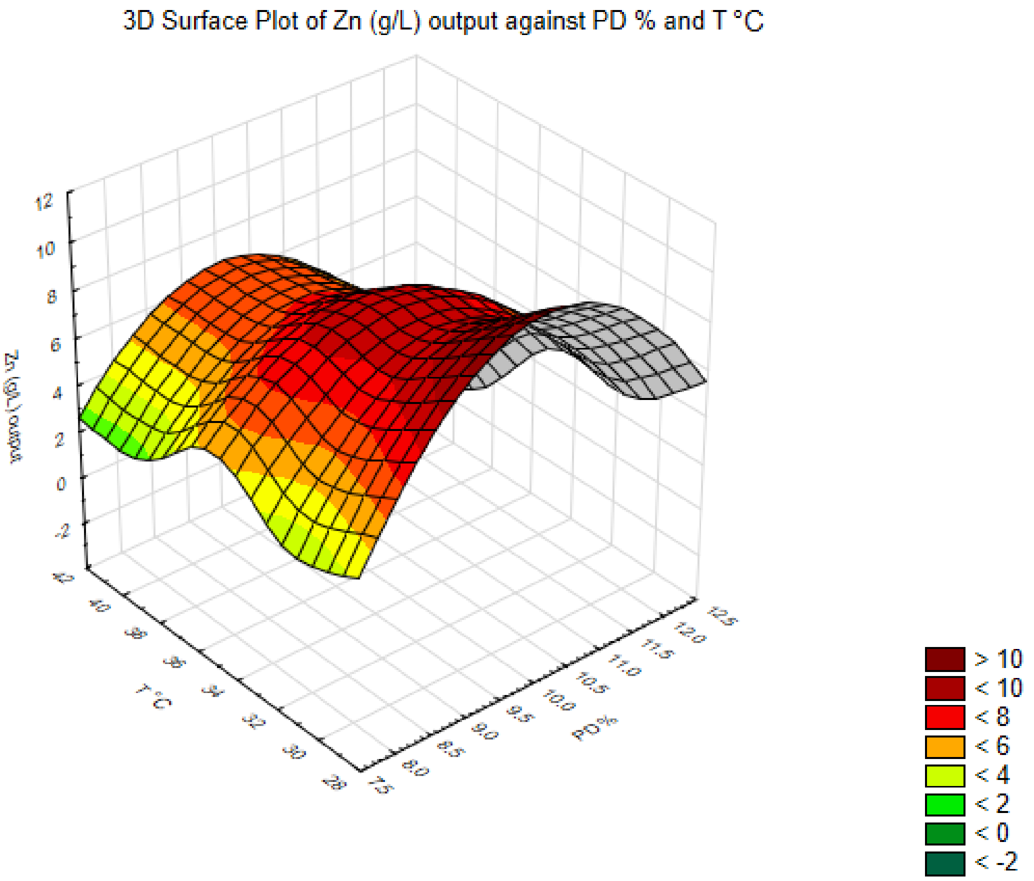
3D Surface Plot of Zn (g/L) output against PD % and T °C
Zn (g/L) output
T °C
PD %
> 10
< 10
< 8
< 6
< 4
< 2
< 0
< -2

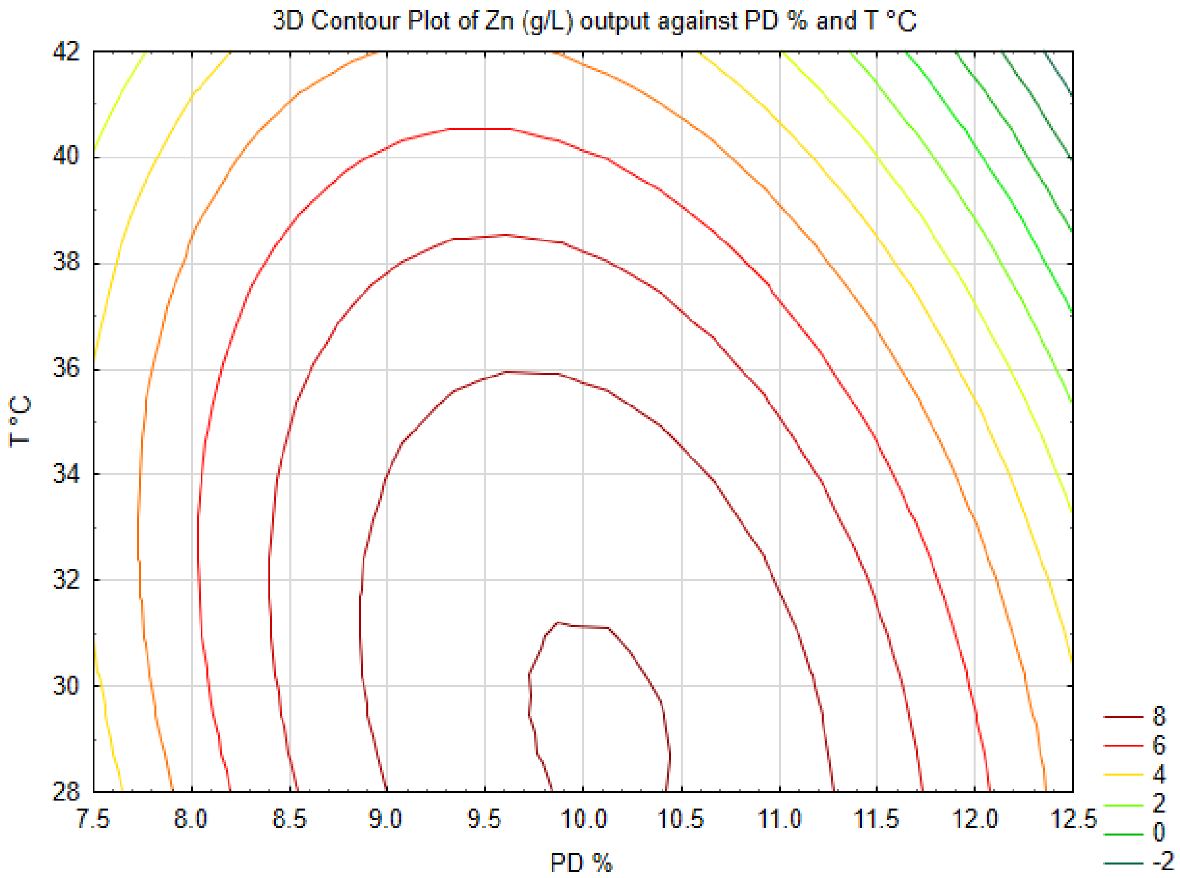

3D Contour Plot of Zn (g/L) output against PD % and T °C
T °C
42
40
38
36
34
32
30
28
7.5
8.0
8.5
9.0
9.5
10.0
10.5
11.0
11.5
12.0
12.5
PD %
8
6
4
2
0
-2

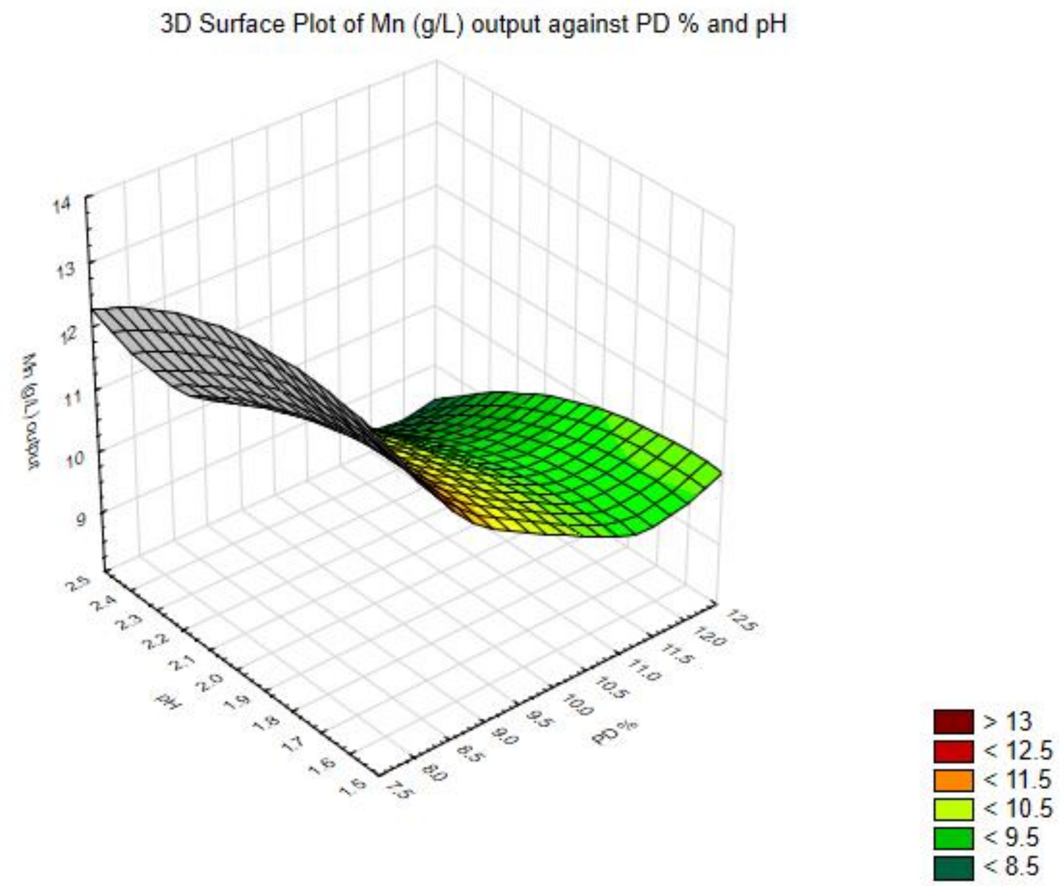
3D Surface Plot of Mn (g/L) output against PD % and pH
Mn (g/L) output
14
13
12
11
10
9
pH
2.5
2.4
2.3
2.2
2.1
2.0
1.9
1.8
1.7
1.6
1.5
PD %
7.5
8.0
8.5
9.0
9.5
10.0
10.5
11.0
11.5
12.0
12.5
> 13
< 12.5
< 11.5
< 10.5
< 9.5
< 8.5

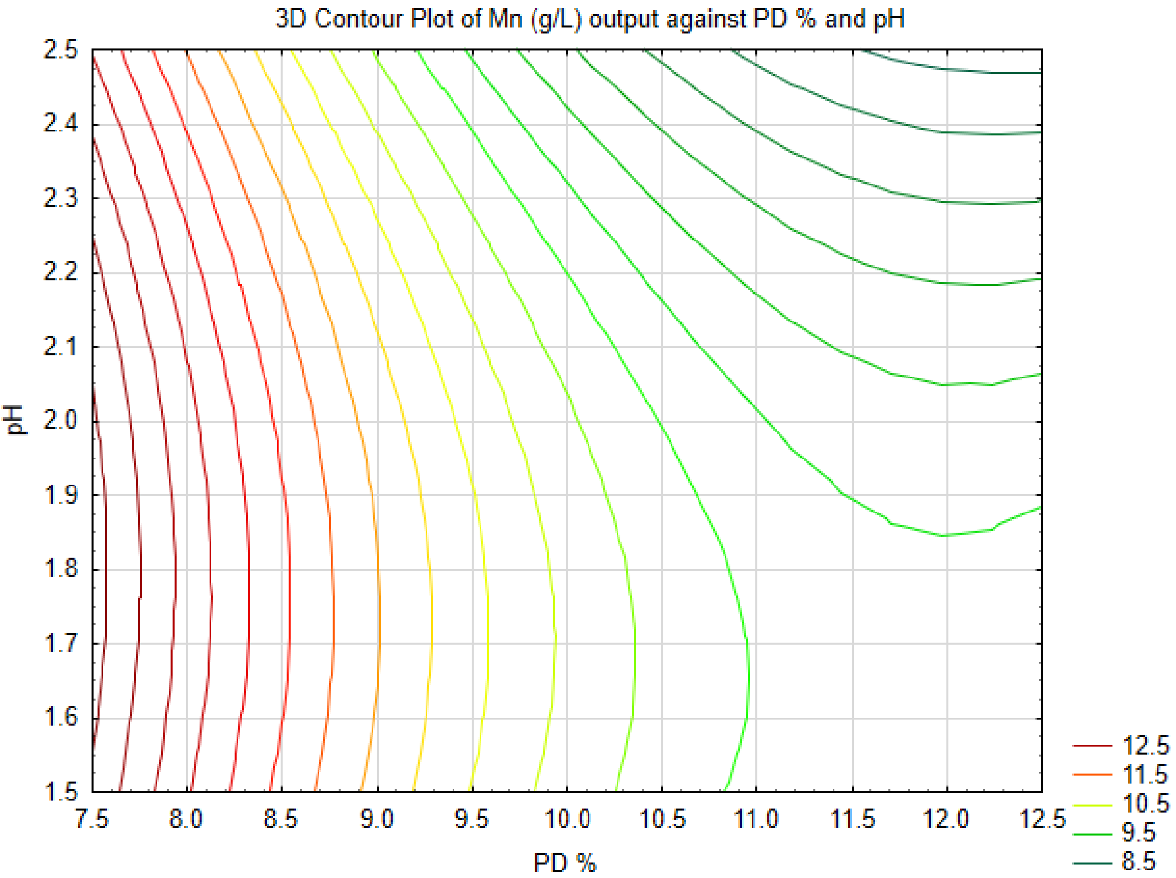
3D Contour Plot of Mn (g/L) output against PD % and pH
pH
2.5
2.4
2.3
2.2
2.1
2.0
1.9
1.8
1.7
1.6
1.5
7.5
8.0
8.5
9.0
9.5
10.0
10.5
11.0
11.5
12.0
12.5
PD %
12.5
11.5
10.5
9.5
8.5